

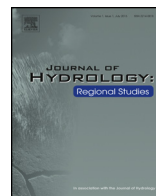


ELSEVIER

Contents lists available at ScienceDirect

## Journal of Hydrology: Regional Studies

journal homepage: [www.elsevier.com/locate/ejrh](http://www.elsevier.com/locate/ejrh)



# Hydrogeology of Montserrat review and new insights



Brioch Hemmings<sup>a,\*</sup>, Fiona Whitaker<sup>a</sup>, Joachim Gottsmann<sup>a</sup>, Andrew Hughes<sup>b</sup>

<sup>a</sup> School of Earth Sciences, University of Bristol, Bristol, UK

<sup>b</sup> British Geological Survey, Keyworth, Nottingham, UK

### ARTICLE INFO

#### Article history:

Received 21 February 2014

Received in revised form 20 August 2014

Accepted 30 August 2014

#### Keywords:

Volcanic island  
Island hydrogeology  
Springs  
Recharge  
Volcaniclastic  
Permeability

### ABSTRACT

**Study region:** The tropical, active volcanic arc island of Montserrat, Lesser Antilles, Caribbean.

**Study focus:** New insights into hydrological recharge distribution, measurements of aquifer permeability, and geological and hydrological field observations from Montserrat are combined with a review of the current understanding of volcanic island hydrology. The aim is to begin to develop a conceptual model for the hydrology of Montserrat, and to inform and stimulate further investigation into the hydrology of volcanic arc islands, by combining a review of the current understanding of essential components of the hydrological system with fresh analysis of existing data, and new observations, data collection and analysis. This study provides new insights into hydrological recharge distribution, measurements of aquifer permeability, and geological and hydrological field observations from Montserrat.

**New hydrological insights for the region:** A new groundwater recharge model predicts whole island recharge of 266 mm/year, between 10% and 20% of annual rainfall. Core scale permeability tests reveal ranges from  $10^{-14}$  to  $10^{-12}$  m<sup>2</sup> for volcaniclastic rocks with coarse matrix, to a minimum of  $10^{-18}$  m<sup>2</sup> for andesitic lavas and volcaniclastics with fine or altered matrix. Analysis of historical pumping tests on aquifers in reworked, channel and alluvial sediment indicate permeabilities  $\sim 10^{-10}$  m<sup>2</sup>. Springs at elevations between 200 and 400 m above mean sea level on Centre Hills currently discharge over 45 L/s. High discharge require a reasonably laterally continuous low permeability body. Contrasting conceptual models are presented to illustrate two potential hydrogeological scenarios. New field observations also reveal systematic spatial variations in spring water temperature and specific electrical conductivity indicating that meteoric waters supplying the springs are mixed with a deeper groundwater source at some sites.

© 2014 The Authors. Published by Elsevier B.V. This is an open access article under the CC BY license (<http://creativecommons.org/licenses/by/3.0/>).

\* Corresponding author. Tel.: +44 117 33 15141.

E-mail addresses: [brioch.hemmings@bristol.ac.uk](mailto:brioch.hemmings@bristol.ac.uk), [briochh@gmail.com](mailto:briochh@gmail.com) (B. Hemmings).

## 1. Introduction

A quantitative understanding of hydrology is important for resource management in all island settings (e.g. Bahamas, [Whitaker and Smart \(1997\)](#); Malta, [Stuart et al. \(2010\)](#)). In many volcanic island terrains, including the Lesser Antilles arc island of Montserrat, high permeability surface geology generates limited and ephemeral drainage systems ([Peterson, 1972](#); [Cabrera and Custodio, 2004](#)). In such environments water supplies often rely entirely on the productivity of springs and abstraction from other parts of the groundwater system.

In active volcanic island settings the involvement of groundwater in volcanic processes can destabilise the edifice and generate explosive phreatic eruptions ([Germanovich and Lowell, 1995](#); [Reid et al., 2001](#); [Fournier et al., 2010](#)). Hydrological systems have also been observed to respond to volcanic perturbations ([Shibata and Akita, 2001](#); [Hurwitz and Johnston, 2003](#); [Kopylova and Boldina, 2012](#)). It is, therefore, possible that the hydrological system may provide valuable information about the state of a restless volcano prior to eruption. [Hautmann et al. \(2010\)](#) proposed that groundwater movement, in response to changes in volcanic activity may be responsible for residual gravity anomalies recorded on Montserrat between 2006 and 2008. The potential for groundwater perturbations to precede an eruption (e.g. Usu, Japan; [Shibata and Akita, 2001](#)) and generate recordable geophysical signals that contain information about active state of a volcano, demonstrates that understanding the hydrological system in volcanic settings is essential for the development and correct interpretation of a truly multi-parameter, hazard monitoring dataset.

Existing conceptual models describing the hydrogeology of small volcanic islands are based on observations from basaltic, ocean island volcanoes, dominated by relatively permeable basalt lava flows. [Cruz and Silva \(2001\)](#) highlight two major and conflicting conceptual models for such settings: the Hawaiian model and the Canary Island model.

The Hawaiian model describes a low-lying, basal water table aquifer with high-level water bodies perched on low permeability ash or soil beds and impounded by dykes ([Peterson, 1972](#); [Ingebritsen and Scholl, 1993](#)). A coastal borehole drilled as part of the Hawaii Scientific Drilling Project in 1993 encountered three freshwater aquifers, each overlying saline to brackish groundwaters, separated by leaky aquitards of soil and ash horizons or calcareous sediments ([Thomas et al., 1996](#)). [Thomas et al. \(1996\)](#) propose that soil layers and extensive ash beds are responsible for elevating inland ground water levels. A borehole drilled at 1102 m amsl, 14 km inland, near the summit of Kilauea volcano, encountered the water table at just 610 m amsl ([Keller et al., 1979](#)). The Hawaiian model has been used to describe the conceptual hydrology of Cape Verde Islands ([Heilweil et al., 2009](#)). This model has also been applied to the Canary Islands, including Tenerife ([Ecker, 1976](#)). However, the current, preferred Canary Island model, considers a single, continuous, water table that domes steeply inland, to high elevation, over low permeability volcanic cores ([Cabrera and Custodio, 2004](#); [Custodio, 2007](#)). The Canary Island model has also been proposed for similar ocean island volcanoes, including Pico Island in the Azores ([Cruz and Silva, 2001](#)) and Reunion Island ([Join et al., 2005](#)).

However, the hydrology of volcanic arc islands is comparatively poorly studied. [Robins et al. \(1990\)](#) identified three island hydrology types in the Lesser Antilles Island Arc, related to the abundance of rainfall and age of deposits. Type 1, based on Grenada and St Vincent, resembles the Canary Island model; a shallow water table doming steeply inland to elevations above 250 m, over a low permeability volcanic core, with springs at all elevations. Type 2 more closely resembles the Hawaiian model, but with the notable absence of impounding dykes. Type 2 is based on the islands of Saint Kitts and Nevis where the younger (Pleistocene) volcanic deposits support perched aquifers of limited capacity and ephemeral streams. Type 3 describes older, Eocene volcanic islands, such as the British Virgin Islands, with exposed low permeability cores and very limited exploitable groundwater potential in low lying alluvial deposits.

Here we review the existing understanding of essential components of Montserrat's hydrological system. This review, which combines published literature and previously unpublished historical data, is supplemented by new observations, data collection and analysis. We provide new insights into hydrological inputs, measurements of aquifer permeability, and geological and hydrological field observations from Montserrat. By combining these new observations and fresh analysis of existing data with our existing understanding of some of the components of the hydrological system, we can

begin to develop a conceptual model for the hydrology of Montserrat. The aim is to improve our fundamental understanding of the hydrology of Montserrat. This will inform and stimulate further investigation into hydrology of volcanic arc islands; in particular, exploration of the coupled hydrological, geomechanical and geophysical feedbacks associated with volcanic and tectonic activity, and assessment of the response of island groundwater resources to a changing climate.

## 2. Geological and geomorphological review

Montserrat is located at the northern end of the Lesser Antilles volcanic arc in the eastern Caribbean (Fig. 1). The island is made up almost exclusively of volcanic rocks erupted from four volcanic centres in three regions. North to south, these are: Silver Hills (SH; 2600–1200 ka), Centre Hills (CH; 950–550 ka) and the Soufrière Hills Volcano (SHV) – South Soufrière Hills (SSH) complex (174 ka to present) (Harford et al., 2002). The progression of activity from north to south and the associated greater erosion of the volcanic centres in the north has formed a tear-drop shaped island approximately 16.5 km north-south and up to 10 km east-west, with an aerial extent of approximately 160 km<sup>2</sup>.

There is no indication of temporal overlap in the activity of the three major volcanic complexes on Montserrat (Cassidy et al., 2012). Consistency between the type of deposits present across the island suggests that the andesitic dome forming style of eruption is common to SH, CH and SHV. The only exception is SSH which possesses basaltic and basaltic–andesite lava flows (Zellmer et al., 2003) and is likely to have some temporal overlap with the early activity of SHV.

The apparent consistency in eruptive style means that the island's volcanic centres provide a unique insight into the temporal evolution of a system, from the building of a complex volcanic edifice (SHV) to the eventual erosion back to the central core and most proximal deposits of an extinct volcano (SH).

The last 15 years of eruption at SHV have been characterised by periods of dome growth and subsequent collapse. The domes grow by extrusion of highly viscous andesitic spines that break off to form blocky, often unstable, talus slopes. Between 1995 and 2009 SHV erupted an estimated 1 km<sup>3</sup> dense rock equivalent (DRE) of andesite magma (Wadge et al., 2010). As the domes grow they can become gravitationally unstable or undermined by slope weakening associated with hydrothermal activity (Sparks et al., 2002). Dome collapses generate volcaniclastic deposits, including clay-rich debris avalanches, pyroclastic flows, surges and lahars (Cole et al., 1998). Collapses have also been triggered by violent vulcanian explosions that produce pumice-rich flows, surges and lahars, as well as significant volumes of ash (Druitt et al., 2002). The resultant geology is characterised by variably fractured, though relatively competent, cores of andesitic dome rock and talus breccia, surrounded by volcaniclastic aprons. These flanking deposits are often referred to as andesite tuffs (Rea, 1974), though they vary in the proportions of andesite lava blocks, pumice and ash. Such geological framework is not uncommon at dome building composite volcanoes (Fisher et al., 2006) and is observed throughout the Lesser Antilles, for example, Guadeloupe, Martinique, Dominica and St Lucia (Sigurdsson et al., 1980).

During periods of repose, erosional forces dominate, expedited by high rainfall, tropical storms and the humid climate (see Section 3). Frequent heavy rain cuts deeply incised radial valleys (locally termed ghauts) and reworks channel fill deposits. Periods of low or no volcanic activity also allow the development of weathered surfaces and soils. Rad et al. (2007) described conglomerate and sand pyroclastic soils, with thicknesses up to 70 m, on the Lesser Antilles islands of Guadeloupe and Martinique. Their study suggests subsurface weathering is considerable, owing to the high permeability and porosity of young pyroclastic deposits. In Costa Rica, Nieuwenhuysen et al. (1993) estimate that well developed andisols form in sandy andesitic parent material within 2000 years. With very similar protolith and climate on Montserrat, soil development is likely to be comparable. Prior to the current eruption of SHV it is thought that the volcano was last active in the early 1600s (Young et al., 1998). It is unclear if 300–400 year activity cycle represents typical behaviour for SHV and Montserratian volcanism in general. Based on the development of erosional unconformities within <sup>14</sup>C dated units (Roobol and Smith, 1998), Harford et al. (2002) propose periods of reduced activity on the order of 10<sup>2</sup>–10<sup>4</sup> years. Although outcrops are limited by vegetation cover on the steep flanks CH, palaeosol layers over 2 m thick can be observed in road cuttings at 230 m above mean sea level (amsl).

Geomorphological difference between the three major volcanic regions on Montserrat reflects the difference in age and erosional maturity from north to south. SH in the north is heavily eroded back to

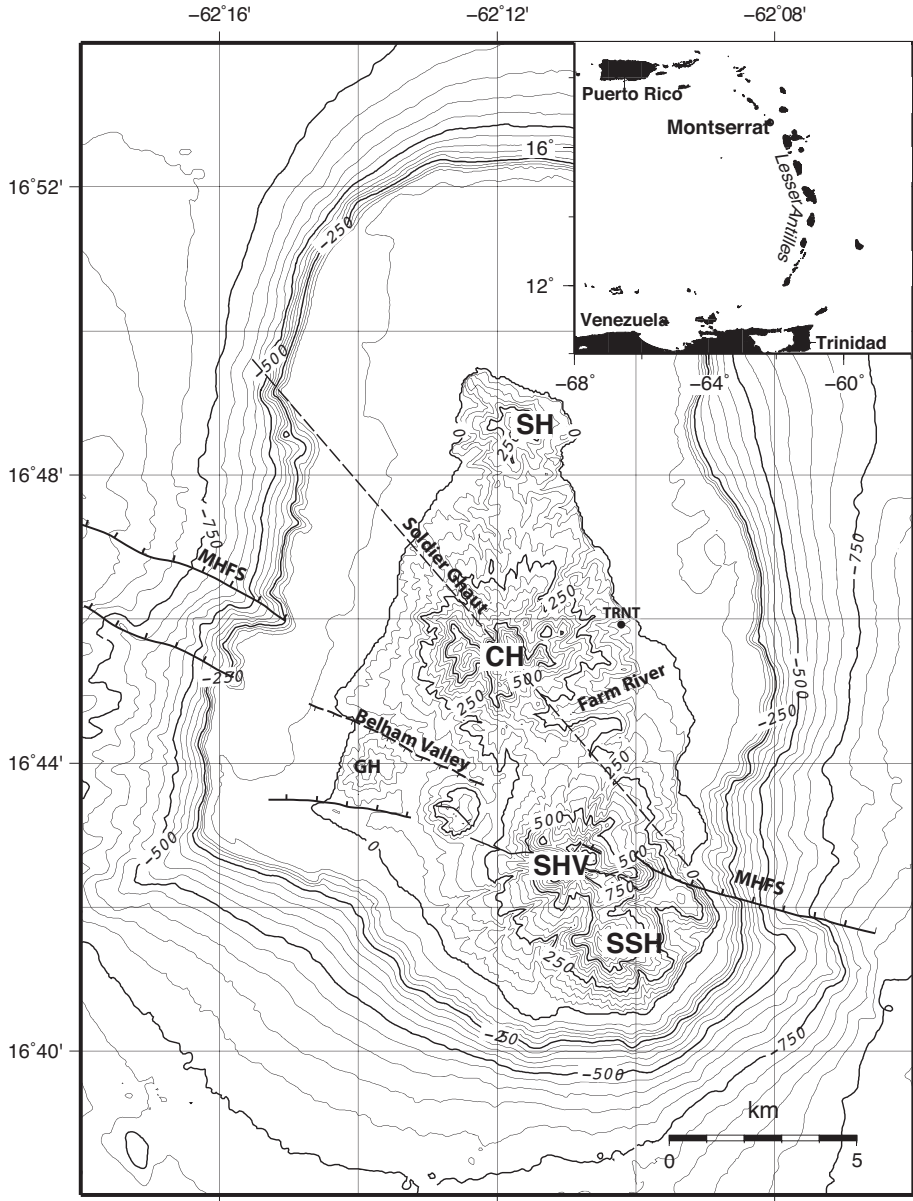


**Fig. 1.** Montserrat and its location within the Lesser Antilles Arc (inset). The major volcanic complexes are labelled: SH, Silver Hills; CH, Centre Hills; SHV, Soufrière Hills Volcano; SSH, South Soufrière Hills. Also marked are GH Garibaldi Hill; SGH, St George's Hill and the major active (solid lines) and inferred (dashed lines) fault systems: MHFS, Montserrat-Havers Fault System and Belham Valley fault from [Feuillet et al. \(2010\)](#); Soldier Ghatt fault, inferred by [Hautmann et al. \(2010\)](#). Also marked is the location of the Trants/Pelican Bay CALIPSO borehole (TRNT).

a distinct steep-sided volcanic core with a maximum elevation of 400 m amsl and a subaerial extent of approximately 7.5 km<sup>2</sup>. The central 35 km<sup>2</sup> of CH is dominated by steep sided intrusive and extrusive components of remnant domes. The highest point in the CH complex is the remnant dome of Katy Hill at 740 m amsl. The steep-sided pinnacles are surrounded by shallower dipping volcanoclastic deposits,

often deeply incised by the modern drainage channels and exposed along coastal cliffs, 140 m high to the east and 75 m high to the west (Le Friant et al., 2004). The morphology of the southern portion of the island has changed noticeably during the most recent activity at SHV. The pre-eruption elevation of SHV was 914 m amsl at the summit of the youngest dome, Castle Peak, which likely dates from early 17th century (Harford et al., 2002). During the phases of dome growth and collapse since 1995 the dome has reached a maximum elevation of 1100 m amsl (Wadge et al., 2010). Major valleys, incised into the volcano's flanks have been partially or completely infilled by deposits from the ongoing eruption (Le Friant et al., 2004) and coastal fans have added significantly to the island's coastline (Cole et al., 2002).

This general morphology of the island sits within a wider, local and regional, tectonic context which reveals itself in a number of on island features as well as in offshore seismic reflection sections (Kenedi et al., 2010). Montserrat is located at the end of the regional Bouillante–Montserrat graben structure between Guadeloupe and southern Montserrat. On the west side of the island normal faulting is prevalent, as part of the extensional Montserrat–Havers Fault System (MHFS) (Feuillet et al., 2010) which manifests as alignment of young andesitic domes and uplift structures and the ESE trending Belham Valley Fault. Further north, Hautmann et al. (2009) have proposed a NW trending fault beneath CH at Soldier Ghaut (Fig. 1). At the more local scale, the shallow intrusive and extrusive lavas that form the cores of the volcanic massifs on Montserrat are pervasively jointed and fractured and small faults can be observed in outcrops exposed by the erosion of the ghaunts. Fractures predominantly strike NW–SE to NNW–SSE with dip angles between 60° and 90° (Hautmann et al., 2010).

### 3. Climate, rainfall and recharge

#### 3.1. Temperature

Montserrat has a subtropical maritime climate. The average annual temperature at sea level is 25.9 °C and average monthly temperatures range between 24 and 27 °C. Temperatures peak in August and are generally lowest in February (Fig. 2). Temperature also varies with elevation. Blume et al. (1974) suggest an average reduction in air temperature of 0.6 °C per 100 m of altitude for the Caribbean islands. Unfortunately, there is not sufficient temperature data to define an independent relationship for Montserrat.

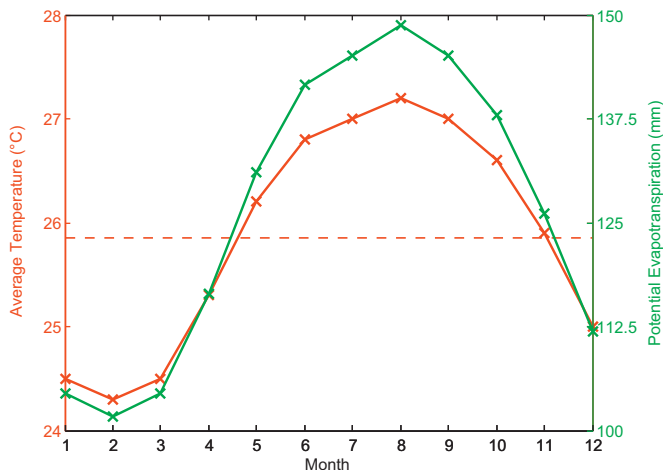


**Fig. 2.** Average monthly temperature at sea level on Montserrat for the period 1990–2009 and monthly potential evapotranspiration given by the Thornthwaite method (see Section 3.3). The dashed red line represents the annual average temperature. Temperature data from Climate Research Unit (CRU) of the University of East Anglia (UEA) via the World Bank Climate Change Knowledge Portal.

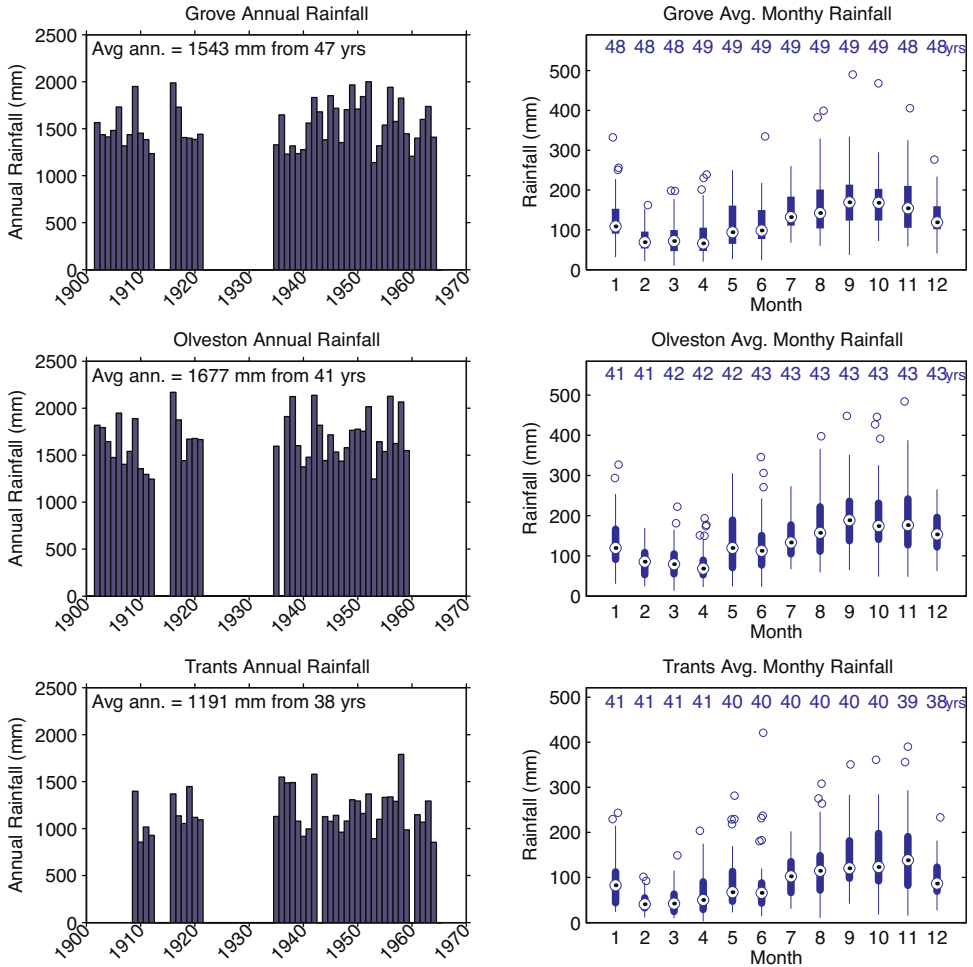


**Fig. 3.** Annual rainfall at Grove, Olveston and Trants from 1905 to 1965 (left). Boxplot of monthly data for the time period covered (right). The boxes define the 25th and 75th percentiles and the dot within the box is the median; the whiskers extend to data points not considered outliers; an outlier is defined as a data value greater than  $q_3 + 1.5(q_3 - q_1)$  and less than  $q_1 - 1.5(q_3 - q_1)$ , where  $q_1$  and  $q_3$  are the 25th and 75th percentiles, respectively. The locations of these stations are highlighted in Fig. 4.

### 3.2. Rainfall

The island experiences both local convective storms and intense rainfall associated with larger tropical weather systems (Barclay et al., 2006). Historical data acquired from the archives of Monserrat Utilities Ltd (MUL) demonstrates that, while rainfall is common throughout the year, a clear seasonality does exist (Fig. 3). The wet season extends from July to November, with rainfall totals decreasing through December and January into a dry season from February to April. The end of the dry season is often marked abruptly by high rainfall through May, before a more steady increase in monthly precipitation to a maximum in the months of September, October and November.

While frequent, year round, high intensity but short (minute-hour) convective storms provide much of the baseline precipitation on the island, tropical storms and hurricanes are responsible for significant additional precipitation associated with the wet season peak. In 2010 Hurricane Earl passed 150 km off the east coast of Montserrat, delivering almost 10% of the recorded annual rainfall at Hope

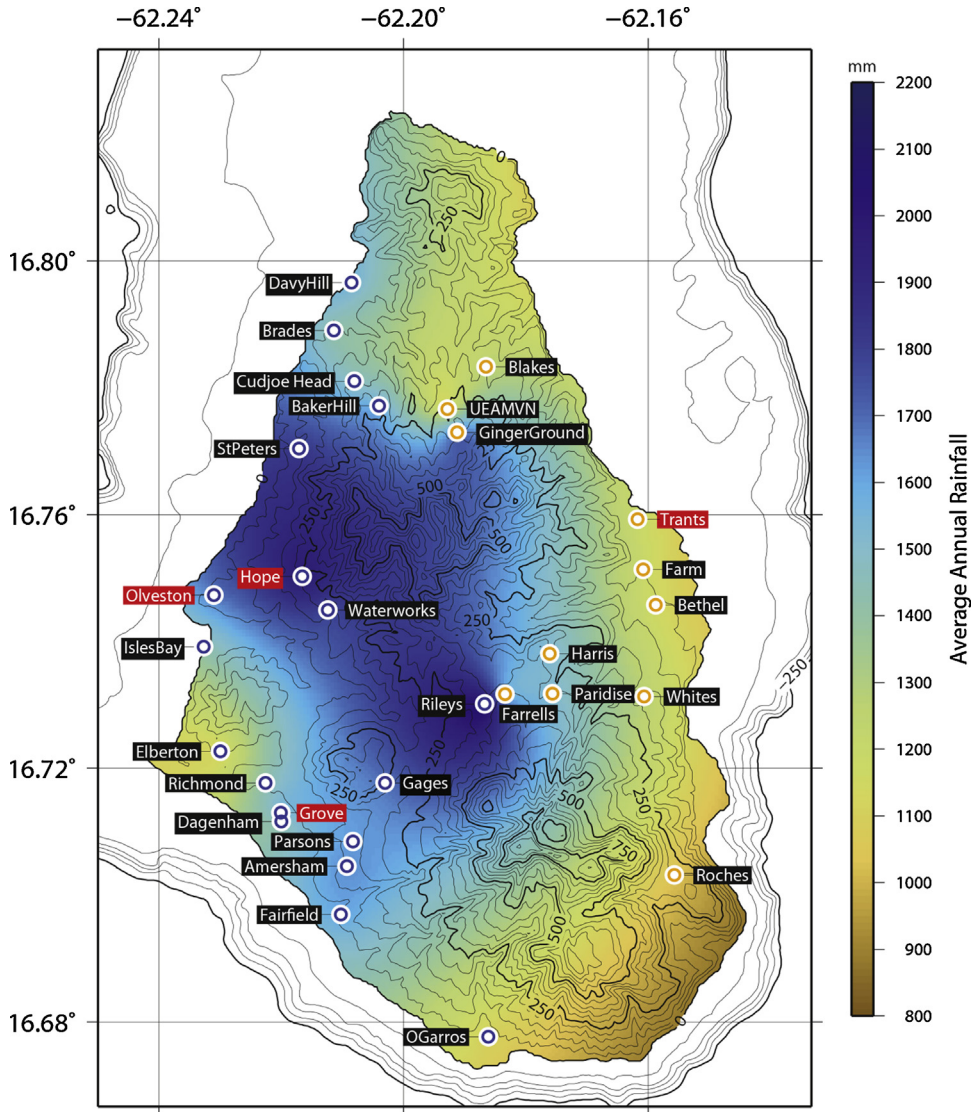


**Fig. 4.** Spatial distribution of average annual rainfall derived from rain gauges with more than 5 years of data. Blue circles correspond to gauges defined as western stations, orange circles are locations of eastern stations (see Fig. 5). Names highlighted in red mark correspond to stations discussed in the text and in Fig. 3.

rain gauge, in just a few hours. There is also significant interannual variation in rainfall on Montserrat, complexly related to sea surface temperatures in the eastern Pacific Ocean (El Nino-La Nina), as well as in the tropical and subtropical Atlantic Ocean (Barclay et al., 2006). Historic data from a pre-eruption rain gauge at Grove in Plymouth (location of rain gauges displayed in Fig. 4) provides monthly totals spanning 47 non-consecutive years between 1902 and 1965. The total annual rainfall for this period ranges from 1139 to 2000 mm with a mean of 1543 mm and standard deviation of 237 mm.

The distribution of precipitation also varies spatially (Fig. 4). Unsurprisingly, on this steep, volcanic island a significant topographic variation in rainfall exists. Barclay et al. (2006) suggested that the mountain tops receive 60% more rainfall than the lower-lying coastal areas. Data from MUL archives,

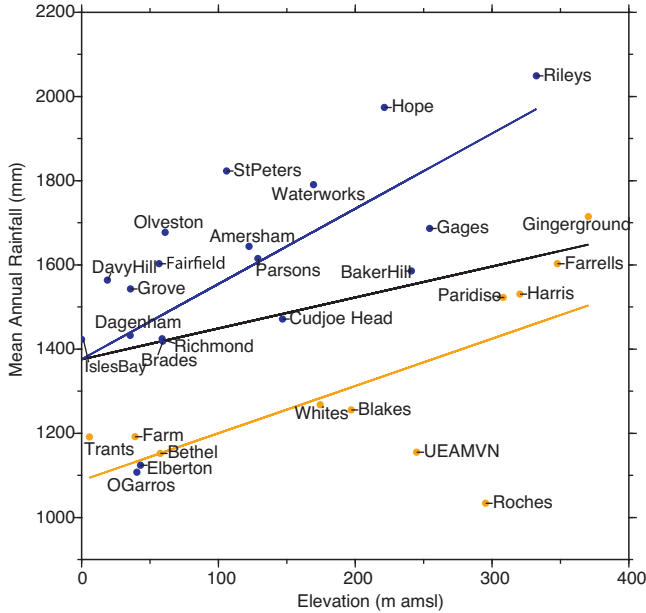


**Fig. 5.** Rainfall relationship with elevation. Station divided into east (orange) and west (blue) locations (see Fig. 4) with different associated rainfall vs elevation relationships. The trend for all 30 stations is described by the equation  $y = 0.734x + 1375.5$  (black line). For western stations the trend is described by the equation  $y = 1.788x + 1375.8$ . The trend for the eastern gauges is  $y = 1.123x + 1087.8$ . Low  $R^2$  values for the east and west relationships (0.48 and 0.43, respectively) indicate the presence of additional spatial rainfall distribution factors as well as temporal variations. However, separate east/west relationships are favourable compared to the complete 30 station trend ( $R^2 = 0.11$ ). Note that the data from the rain gauges cover different time periods within the interval 1900–2011 (average length of data set is  $21 \pm 13$  years).

supplemented by a single station from a University of East Anglia (UEA) instrumentation show that the topographically controlled distribution is coupled with a distinct east-west contrast. Rainfall is higher on the leeward (western) side of the island, especially on the western slopes of Centre Hills (Fig. 4). There is also a contrast in the relationship between elevation and rainfall in the east and west of the island (Fig. 5). The available rain gauge data suggest that rainfall is ~80% greater over the eastern peaks than on the coast; in the west it is >100% greater on the peaks. A paucity of instrumentation within the densely vegetated high elevation regions restricts the accuracy of this estimate. The spatial variation in precipitation is reflected in climax vegetation; the leeward (western) and elevated areas that are unaffected by the volcanic activity are covered in dense, tropical forest, while scrub, grass and cacti dominate the dry, windward (eastern) and northern slopes and coast.

### 3.3. Recharge estimation

Groundwater recharge is a critical control on any subsurface hydrological system. In tropical islands such as Montserrat, high temperatures and dense vegetation can combine to produce high evapotranspiration rates, significantly reducing effective recharge. No evaporation pan measurements exist on Montserrat. In the absence of direct measurements, calculation of the potential evapotranspiration ( $PE_T$ ) is necessary. The Thornthwaite method (Thornthwaite, 1948) is one of the most commonly used of several empirical methods or used to estimate  $PE_T$  (see Schwartz and Zhang, 2003). The method uses average monthly temperature to calculate an estimate for monthly  $PE_T$ .

$$PE_T = 1.62 \left( \frac{10T_{ai}}{I} \right)^a \quad (1)$$

**Table 1**Values for root constant (*C*) and wilting point (*D*) for vegetation types used in the recharge modelling.

Landuse	Root constant (cm) ( <i>C</i> )	Wilting point (cm) ( <i>D</i> )
Tree-dominated	150	250
Bare soil	2	5
Grass-dominated	30	60
Fresh volcanic deposits	2	5

where  $PE_T$  is potential evapotranspiration in cm/month,  $T_{ai}$  is the mean air temperature in °C for month  $i$ .  $I$  is the annual heat index given by:

$$I = \sum_{i=1}^{12} \left( \frac{T_{ai}}{5} \right)^{1.5} \quad (2)$$

from which the constant  $a$  is derived:

$$a = 0.492 + 0.0179I - 0.0000771I^2 + 0.000000675I^3 \quad (3)$$

Thornthwaite estimates for  $PE_T$  on Montserrat vary between 100 and 150 mm/month, yielding a total 1500 mm/year (Fig. 2). Thus  $PE_T$  is close to, and sometimes greater than, the average annual rainfall in some locations. Only when soil water is not limited can actual evapotranspiration ( $AE_T$ ) be assumed to equal  $PE_T$ .

### 3.3.1. The distributed recharge model

We use distributed recharge model code ZOODRM (Hughes et al., 2008; Mansour et al., 2011), to estimate spatially and temporally distributed  $AE_T$  from Thornthwaite  $PE_T$  calculations, by incorporating distributed, daily precipitation data and vegetation type information. We define four vegetation types based on land use maps from the Government of Montserrat: bare soil, grass-dominated (often anthropogenic), tree-dominated and fresh volcanic deposits (Fig. 6). ZOODRM uses a soil moisture deficit (SMD) calculation to relate  $AE_T$  to the  $PE_T$  estimates in Fig. 2 and derive distributed recharge. Two major, depth related parameters are assigned to each vegetation type; the root constant ( $C$ ) and wilting point ( $D$ ) (Table 1). While SMD is less than  $C$ , water in the soil is assumed to be freely available for evapotranspiration. Under these conditions  $AE_T$  is equal to  $PE_T$ . If evapotranspiration continues in the absence of sufficient recharge, SMD increases beyond  $C$  and the amount of moisture that can be extracted from the soil is restricted. If SMD continues to increase beyond the wilting point ( $D$ ) evaporation from soil moisture will cease. If rainfall is greater than  $PE_T$  it will first replenish the SMD before recharge is permitted. The model domain is discretised into nodes, represented by  $200 \text{ m} \times 200 \text{ m}$  cells; daily recharge is calculated for each node following the method summarised in Fig. 7.

The robustness of the recharge model is improved by greater spatial and temporal constraints on the inputs, for instance the length of the daily rainfall time series and the number of rain gauge stations. Although there are long historical monthly time series for precipitation, the longest continuous daily time series is 13 years at Hope rain gauge (Fig. 8). ZOODRM allows the rainfall data to be spatially distributed according to additional known constraints. Here, we evaluate three precipitation distribution scenarios that combine the time series from Hope with information on spatial distribution from the other rain gauges in the network (see Table 2).

### 3.3.2. Recharge modelling results

The predicted average annual recharge ranges from 12.5% to 17.9% of annual average precipitation (Fig. 9). Results from Model 1, where rainfall is spatially homogeneous, suggest that recharge is almost 5 times higher on bare soils and volcanic deposits than on forested regions. While this effect is subdued by the spatial distribution of rainfall used in the more complex models (2–4), land use remains the dominant control on groundwater recharge. The recharge model results are also affected by spatial variation in  $PE_T$ . Model 4 incorporates distributed temperatures based on cooling with elevation at a

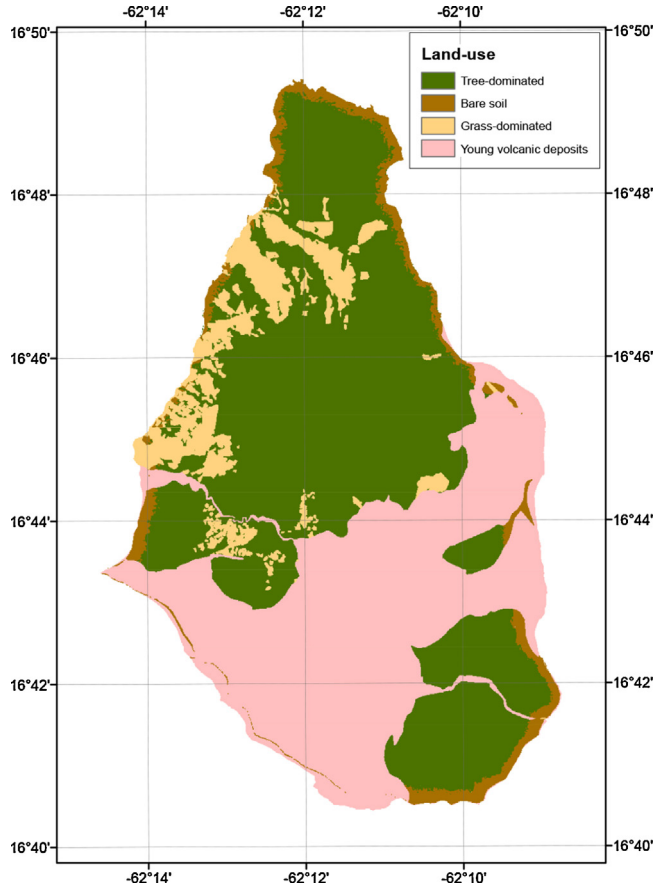


**Fig. 6.** Land-use divisions used in recharge modelling. Land-uses and vegetation types simplified from Government of Montserrat land-use data. Much of the grass-dominated land on the west is anthropogenic, associated with gardens.

**Table 2**

Description of the three rainfall distribution models explored during the development of a recharge model for Montserrat.

Rainfall distribution model	
Name	Description
Uniform	Daily precipitation time series for Hope rain gauge, uniformly distributed.
Elev.: whole island	Precipitation scaled by elevation according to the line of best fit through annual average precipitation vs elevation for all 29 stations with more than 5 years of rain gauge data (all stations in Fig. 5).
Elev.: east/west	Precipitation scaled by elevation according to two relationships that depend on longitude. Eastern cells are scaled by relationship described by line of best fit through the 11 eastern stations (orange stations in Fig. 5). Western cells scaled according to line of best fit through the 18 western stations (blue stations in Fig. 5).

rate of  $-0.6^{\circ}\text{C}/100\text{m}$  (Blume et al., 1974), giving an estimated annual recharge of 266 mm/year (16.7% of mean annual rainfall).

Temporal variations in groundwater recharge are also significant. Monthly recharge rate estimates for Model 4 are presented in Figs. 10 and 11. October is the wettest month in the Hope rain gauge reference time series (1999–2012, Fig. 8). The rainfall distribution model used in Model 4 predicts a whole island average daily rainfall of 7.77 mm for October, compared to 2.29 mm for the driest month

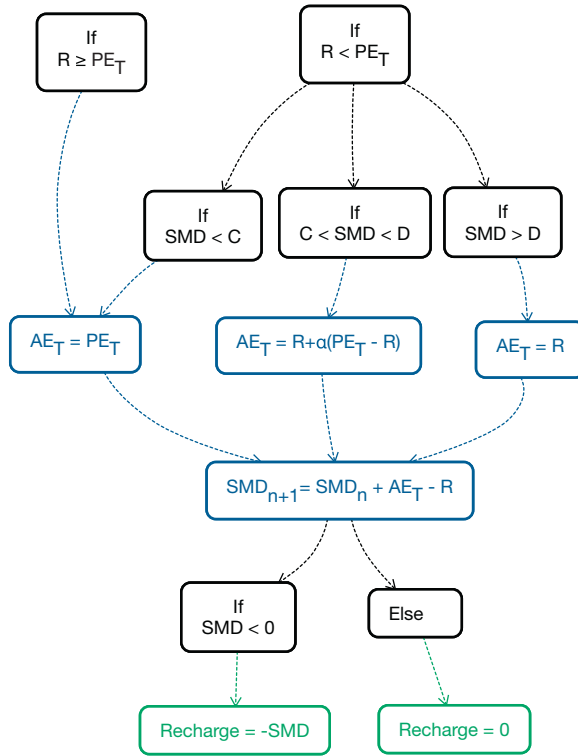


**Fig. 7.** The soil moisture deficit (SMD) method used for each node in the recharge models at each daily time step ( $n$ ).  $R$  is rainfall. The factor  $\alpha$  determines the amount of water lost from the ground when SMD is between the root constant ( $C$ ) and wilting point ( $D$ ).  $PE_T$  and  $AE_T$  are potential and actual evapotranspiration, respectively. For these models we use a value of  $\alpha = 0.1$ .

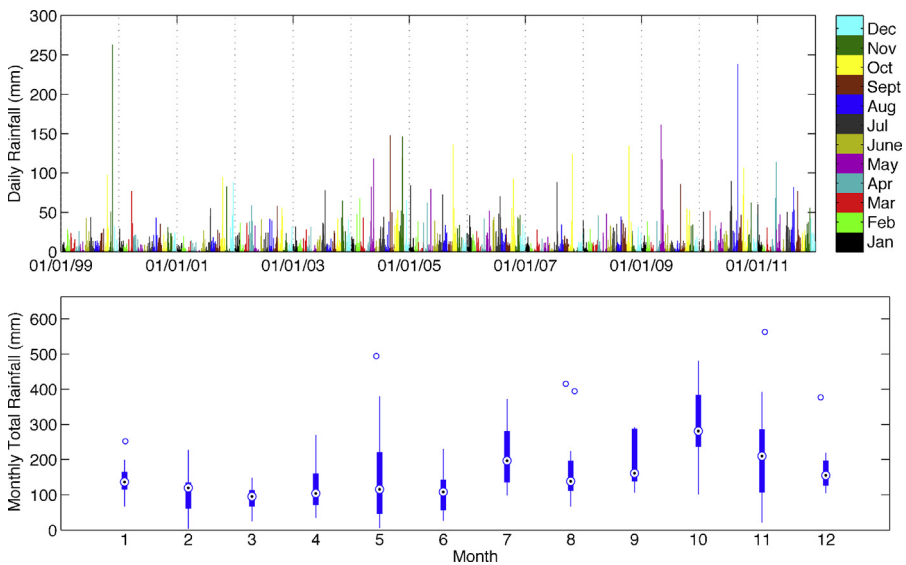


**Fig. 8.** Above: Hope rainfall time series used as reference station for ZOODRM recharge model. Below: monthly box plots for the 13 years of continuous data from Hope. Boxes, whiskers and outliers defined as in Fig. 3.

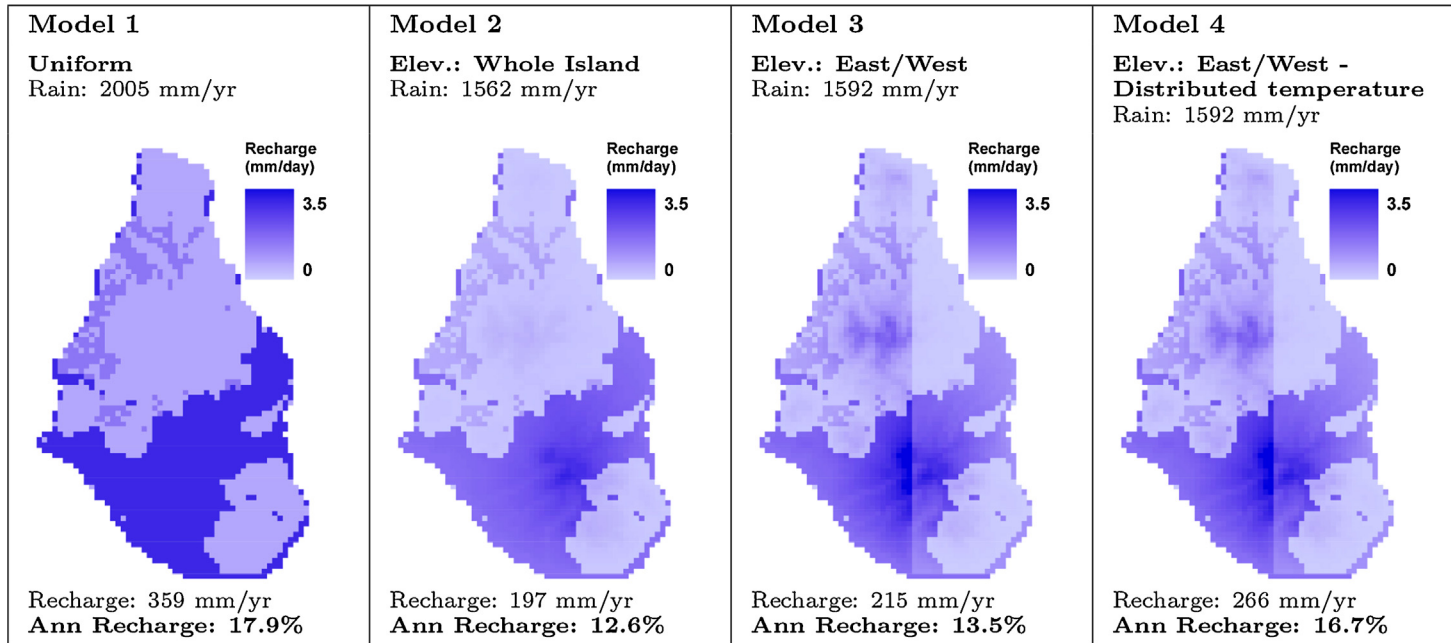


**Fig. 9.** Recharge distribution for the different rainfall and land use scenarios explored. Rainfall models are defined in Table 2. Land use, soil moisture deficit parameters defined in Table 1. Whole island, annual, rainfall and recharge averages are also presented, as well as an estimate of annual recharge percentage. Model 1 demonstrates the land use control on uniformly distributed rainfall and evapotranspiration. Models 2 explores a single, whole island precipitation and elevation relationship. Compared to Model 3 which incorporated different rainfall and elevation relationships for the eastern and western sides of the island, Model 2 underestimates the recharge in the west and overestimates the recharge in the east. Model 4 includes an additional elevation/temperature control on evapotranspiration, with the effect of slightly reducing recharge.

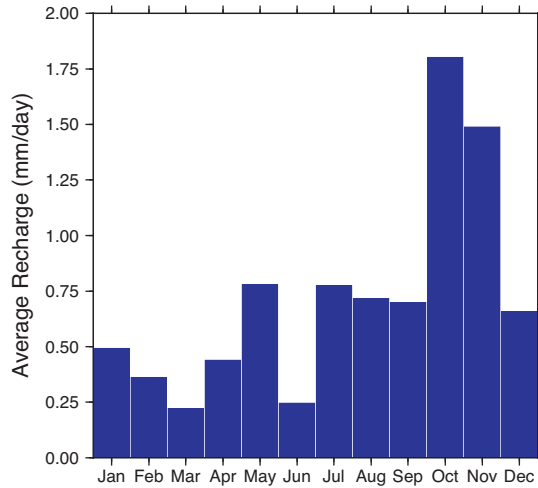


**Fig. 10.** Mean daily recharge for each month predicted by Model 4. The spatial distribution of this recharge can be seen in Fig. 11.

(March). This, coupled with the cumulative effect of increased rainfall lowering SMD during the wet season, results in long term average daily recharge estimate for October that is over 8 times that for March.

### 3.3.3. Recharge model interpretation and discussion

The scenarios investigated here are simplifications of the complex recharge regime on Montserrat. The models attempt to incorporate the spatial relationships of rainfall with elevation and latitude. However, limited daily rainfall time series, particularly at higher elevations, prevents the inclusion of higher order rainfall distribution trends. This will result in overestimation or underestimation of recharge in locations where rainfall does not fit the elevation trends used. A lack of spatially and temporally distributed temperature or evaporation data also restricts the absolute accuracy of the models. However, the models demonstrate that land use is a key control on recharge and as such they provide reasonable first-order estimates of groundwater recharge on Montserrat.

The annual recharge percentages can be compared with the values of 10% and 40% calculated for the nearby islands of Guadeloupe and Martinique, respectively, by Rad et al. (2007), who emphasise 'huge' local variations. Model 4, which attempts to capture the disparity between precipitation on the east and west of the island, as well as temperature variation associated with elevation, represents our best estimate of the true recharge conditions on Montserrat.

The temporal variation captured by these recharge models is purely a function of climatology. Land use (i.e. vegetation type) has a strong influence on the spatial distribution of groundwater recharge and can also vary temporally. Seasonal vegetation variation is negligible in Montserrat's tropical climate. However, vegetation changes associated with waxing and waning of volcanic activity, and deforestation for agriculture and development may systematically affect recharge. These effects are not incorporated in the current recharge models. Generally, over the 13 years covered by the rainfall data (1999–2012), land use has varied little. However, ash from SHV has, at times, covered large parts of the island. Since 2010 the vegetation in the south of Montserrat has begun to recover, during an extended period of quiescence. Development, and particularly agriculture, is also increasing in response to reduced volcanic activity. Future studies should incorporate changes in vegetation associated with recovery and development.

Another important factor not taken into account in this suite of recharge models is the effect of run-off. Unfortunately, the absence of stream hydrograph data on Montserrat means run-off is impossible to quantify. Although measurements suggest that infiltration rates on Montserrat are high

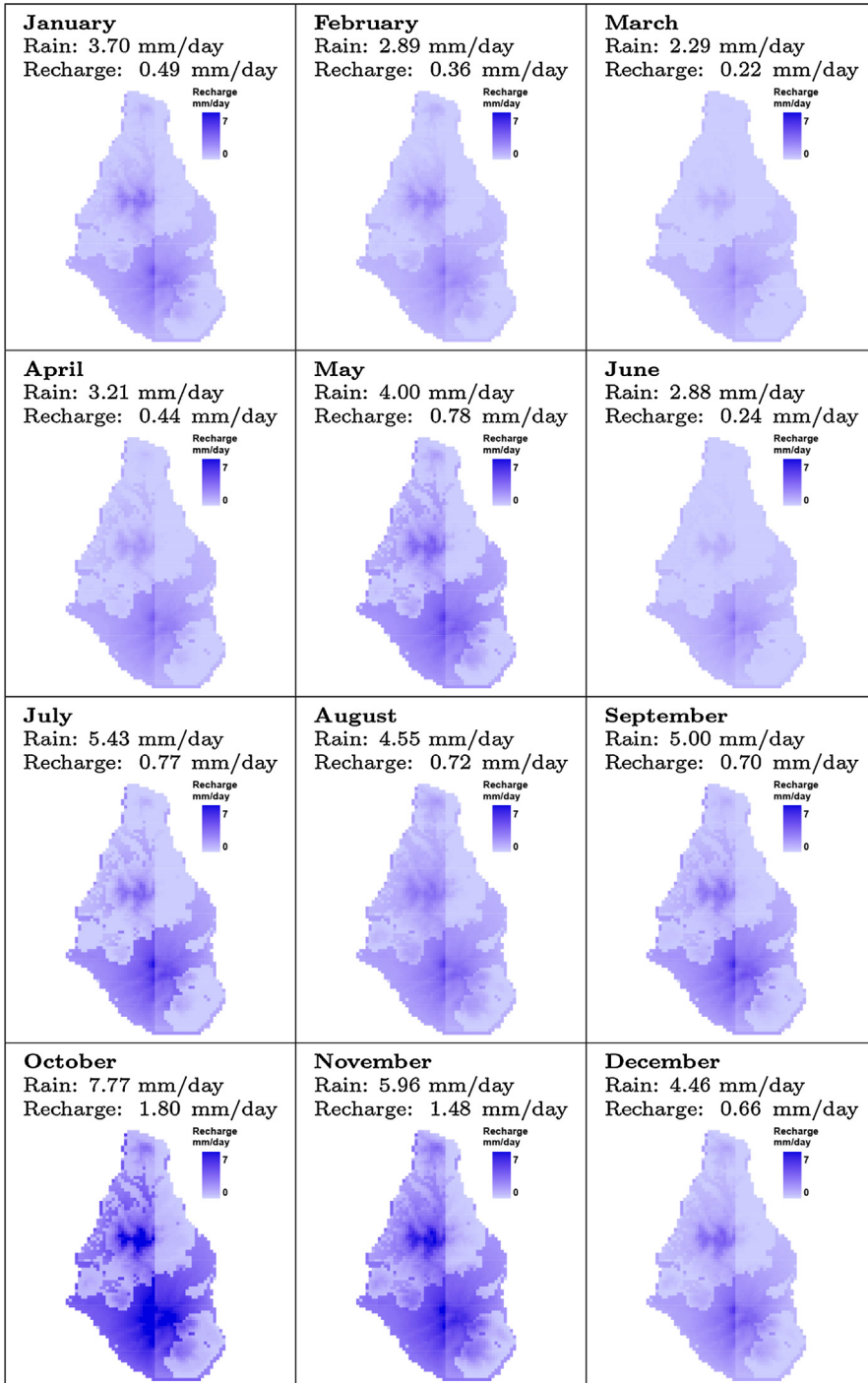


**Fig. 11.** Distribution of mean daily recharge each month, predicted by Model 4 (see Fig. 9). For reference, the whole island, mean daily rainfall and recharge for each month are also quoted.

(>0.75 mm/min) (Barclay et al., 2007), rainfall intensities during storms can exceed this, reaching 2 mm/min. Interception by densely vegetated canopy, moderates the rate at which rainfall reaches the ground. Observations indicate that storm events do generate run-off on steep slopes, however flow rapidly infiltrates into stream beds downstream. As a result run-off on Montserrat predominantly acts to redistribute recharge downstream rather than removes it completely from the groundwater system; only the most intense storms, associated with tropical cyclonic activity, generate run-off to the sea. From measurements of river discharge, Rad et al. (2007) estimate run-off at 60% and 30% of annual precipitation for Guadeloupe and Martinique, respectively. These estimates, which include contributions to river run-off from springs and groundwater aquifer discharge, are not appropriate for use in recharge models. Regardless, such high values are probably greatly excessive for Montserrat where no permanent rivers exist. For the purposes of the recharge models presented here, no run-off was generated.

## 4. Hydrology

### 4.1. Spring discharge and water supply

Despite high rainfall on Montserrat, the network of deeply incised radial valleys (ghauts) that drain the island's steep flanks are predominantly ephemeral. The only permanent streams are sourced from springs at elevations between 200 and 400 m (amsl) (Figs. 12 and 13). The springs feed losing streams;

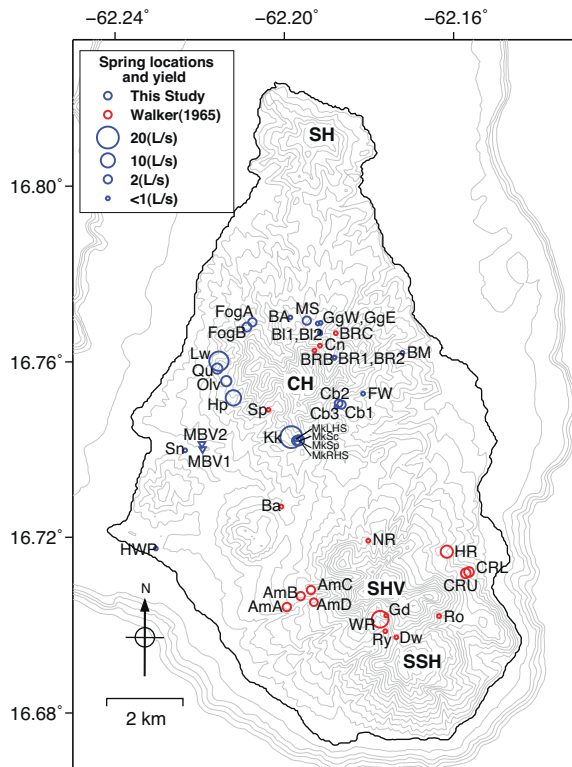


**Fig. 12.** Location and average yield of springs. Blue circles and triangles are spring and well locations with yield data from this study. Red circles are data from Walker (1965). The springs on SHV are no longer accessible and have almost certainly been buried by deposits from the ongoing eruption. Spring names from this study are shown in Table 3; spring names from Walker (1965) study are provided in Appendix A. More detail on spring yields is shown in Fig. 14.

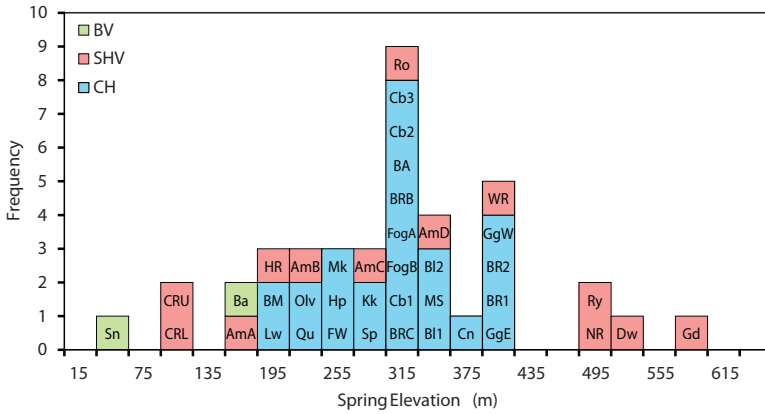


**Fig. 13.** Spring elevation distributions on Centre Hills (CH (blue)), Soufrière Hills Volcano (SHV (red)) and Belham Valley (BV (green)). Bins are 30 m. The lowest elevation spring is Sunny Spring (Sn) at 15 m amsl. CH springs are between 188 and 403 m amsl.

flow infiltrates into the stream bed and flows to the sea as groundwater. There are a few broader drainage channels, such as the Belham and Farm Rivers, to the east and west respectively, between CH and SHV, and Carr’s and Little Bays in the north of the island. Aquifers within major drainage valleys and in alluvial sediments in the vicinity of the old capital, Plymouth, have been explored for groundwater water production in the past, with varying degrees of success (Ramdin and Hosein, 1995; Maxim Engineering, 1995; Davies and Peart, 2003). Most of the wells were shallow (<50 m) and low yielding (<2 L/s) (Davies and Peart, 2003).

Prior to the onset of eruptive activity in 1995 (see Section 2), the water demand of the population of approximately 11,000 was met by selected springs on both CH and SHV (Fig. 12), supplemented by a number of variable quality (chemistry and yield) wells. Concern over declining spring production in the early 1990s, and increasing occurrence of high chloride levels in the more coastal well waters

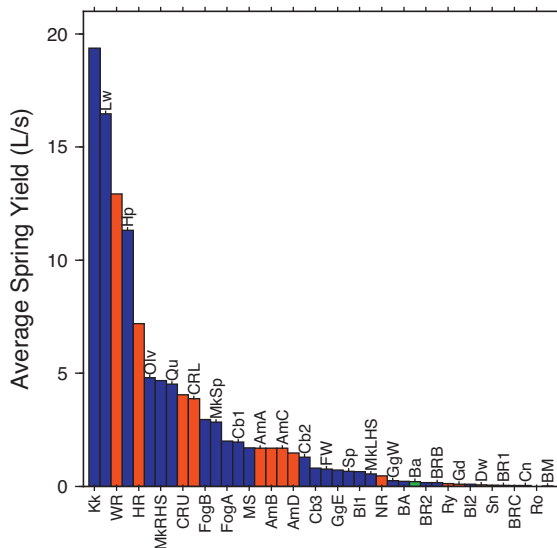


**Fig. 14.** Ranked, average spring yields, from this study and from Walker (1965). CH springs in blue; SHV springs, red and the two springs in the Belham Valley (Sunny (Sn) and Bath (Ba)), green.

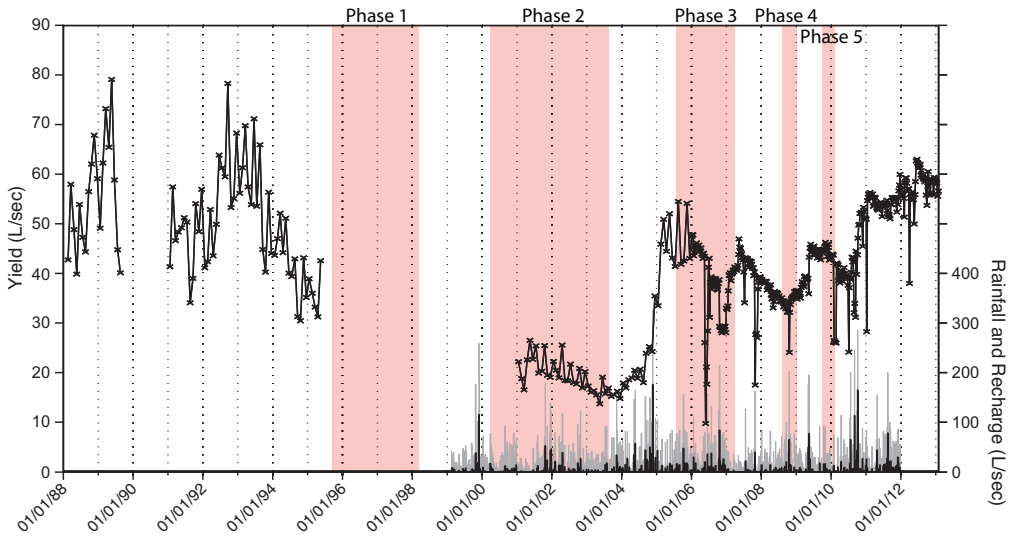


**Fig. 15.** Spring yield from supply springs from 1988 to 2013 according to Montserrat Utilities Ltd (MUL) production data, showing significant fluctuations in spring yields. The early part of the time series is composed of monthly data; weekly data is available from 2006 onwards. The time series is disrupted by Hurricane Hugo from 1989 to 1991 and then by the eruption of SHV between 1995 and 2001. The distinct eruptive phases of SHV are displayed for reference. Projected whole island, weekly rainfall (grey) and recharge rate (black) from Hope rain gauge and Recharge Model 4 are also shown.

prompted investigation into the potential for further groundwater development. Six wells were drilled in the Belham Valley in 1996; one demonstrated artesian flow at 1 L/s and provided a pumped yield of 3.9 L/s (Davies and Peart, 2003). Like many of the valleys in the south on Montserrat, Belham Valley has been inundated with lahars and pyroclastic deposits since the onset of eruptive activity at SHV. In 2007, fill accumulation from lahars in the lower Belham Valley since 1995 was estimated to be between 10 and 15 m (Donnelly, 2007). By 2003, after 8 years of volcanic activity, all wells in the Belham as well as springs on SHV were lost, buried under the young volcanoclastic and lahar deposits from SHV. Abandonment and infilling also took all the other wells out of supply.

In 2004 HydroSource Associates managed a project drilling three wells targeting the productive, artesian aquifer in the Belham Valley (MBV1 and MBV2 in Fig. 12) (HydroSource, 2004). The three wells tap a confined aquifer in reworked gravels and alluvial deposits between 15 and 38 m below mean sea level, confined by a thin (1 m) cap of low permeability clay and lahar deposits beneath a thicker (12 m) lahar deposit. However, as access to these wells is limited during times of heightened volcanic activity and extreme rainfall events, the Belham wells are maintained as a back-up water supply.

Emigration as a result of both hurricane Hugo in 1989 and the onset of volcanic activity in 1995 has reduced Montserrat's population to 4500, easing pressures on the water supplies. The current demand of ~14 ML/week is met by production from six springs on flanks of the extinct volcanic centre of Centre Hills. In 2012 supply from these springs averaged 35 ML/week; excess discharge flows down the ghauts and percolates through the beds of the losing stream. Consumption rates are expected to rise as population and agriculture continue to recover during periods of reduced volcanic activity. While current spring yields provide a surplus and can cope with significant increases in demand, historical variations in spring yield provide some cause for concern. Anecdotal evidence (MUL, pers. commun. 2012) suggests that spring behaviour is affected by volcanic activity. Spring production data suggests that yield declined significantly in the 18 months prior to the onset of the eruption and remained low for ten years. In the early 2000s, during a prolonged period of activity (Phase 2, Fig. 15), spring production declined to levels below the current consumption rate, reaching yields less than 12 ML/week in 2003. Low yield behaviour ended abruptly at the end of Phase 2, with a sudden

**Table 3**

Temperature and SEC of springs surveyed in February 2013. Spring code refers to the labels in Fig. 12.

Spring code	Spring name	Lat. (° N)	Lon. (° W)	Alt. (m)	Date	Temp (°C)	SEC (µS/cm)
BA	Blackwood Allen	16.77010	62.19862	315	10/02/13	23.6	458
Bl1	Bottomless Ghaut 1	16.76671	62.19159	332	04/02/13	22.1	554
Bl2	Bottomless Ghaut 2	16.76642	62.19151	356	04/02/13	22.1	255
BM	Bessy Mack	16.76202	62.17215	190	11/03/13	25.4	1288
BR1	Big River 1	16.76012	62.18815	398	04/02/13	22.7	331
BR2	Big River 2	16.76012	62.18815	398	04/02/13	22.1	353
Cb1	Corbett 1	16.75026	62.18652	306	02/02/13	25.2	467
Cb2	Corbett 2	16.75049	62.18717	325	02/02/13	26.1	423
Cb3	Corbett 3	16.74971	62.18773	327	02/02/13	26.9	419
FogA	Fogarty A	16.76897	62.20753	309	18/02/13	22.8	287
FogB	Fogarty B	16.76789	62.20887	306	18/02/13	22.9	283
FW	Fairy Walk	16.75269	62.18141	248	02/02/13	28.8	555
GgE	Gingerground East	16.76885	62.19141	392	10/02/13	22.5	415
Hp	Hope	16.75177	62.21206	262	08/02/13	23.7	306
Kk	Killiekrankie	16.74284	62.19839	297	31/01/13	25.9	308
Lw	Lawyers	16.76014	62.21544	188	30/01/13	23.2	281
MkSc	Monkey Spring	16.74200	62.19714	265	31/01/13	25.7	311
MkSp	Monkey Spring	16.74200	62.19714	265	31/01/13	26.3	327
MkLHS	Monkey side spring	16.74234	62.19725	297	31/01/13	24.6	326
MkRHS	Monkey side spring	16.74206	62.19656	296	31/01/13	22.2	967
MS	Mongo/Underwood	16.76938	62.19469	345	09/02/13	23	588
Olv	Olveston	16.75557	62.21368	240	05/02/13	23.2	282
Qu	Quashie	16.75845	62.21587	231	30/01/13	23.2	285
Sn	Sunny	16.73979	62.22347	15	06/02/13	27.4	1703
HWP1	Hot Water Pond seaward	16.71748	62.23039	1.0	07/02/13	40.4	49,100
HWP2	Hot Water Pond up-valley	16.71748	62.23039	1.5	07/02/13	56.1	38,600
MBW1	Belham Well 1	16.74009	62.21932	34	06/02/13	31	663
MBW2	Belham Well 2	16.74130	62.21948	29	06/02/13	31	630

production increase to over 25 ML/week (Fig. 15). However, as the spring production data reflects natural recharge fluctuations as well as infrastructure disruptions, establishing a causal link between volcanic activity and spring yield is difficult. Spring yield fluctuations highlight the fragility of this essential resource and underline the need to understand the controls on Montserrat's hydrological system.

#### 4.2. Hydrological field observations

Volcanic activity has buried the spring on SHV. Currently, all of the island's freshwater is supplied by six springs on CH. There are also a number of untapped springs on CH. Previous studies (Chiodini et al., 1996; Davies and Peart, 2003; Jones et al., 2010) have suggested uniformity in temperature and composition of the CH springs. However, measurements of temperature and specific electrical conductivity (SEC) during field campaigns in February and November 2011 and February 2013 indicate differences between CH springs that merit further attention.

The majority of springs on CH, particularly the western and northern springs, discharge water at 22–24 °C and 281–353 µS/cm (Table 3). However, a number of springs on CH produce water above 25 °C. These warmer springs lie in a north-east linear trend and include the high yielding (19 L/s) and high elevation (297 m amsl) supply spring of Killiekrankie (Kk) (at 25.9 °C), on the southern flank of CH, and the low yield (0.01 L/s) and relatively low elevation (190 m amsl) Bessy Mack (BM) (at 25.4 °C) towards the island's east coast (Fig. 16). The highest temperature recorded is at the previously unreported low yielding (~0.8 L/s) Fairy Walk (FW) where spring waters approach 29 °C.

At Sunny Spring (Sn) on the edge of the Belham Valley, below Garibaldi Hill, less than 1 km from the coast at just 15 m amsl (Fig. 12), the spring temperature is also higher than at the northern and western CH springs, discharging at 27.4 °C. Here, water flows from a boggy spring with an estimated discharge of less than 0.1 L/s and a high SEC of 1703 µS/cm (Table 3).

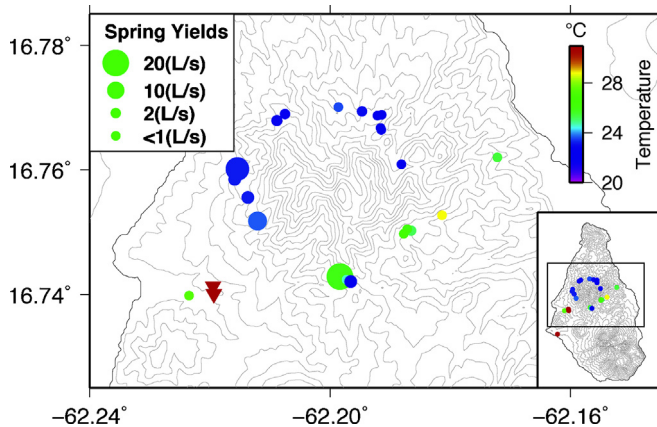


**Fig. 16.** Temperatures of CH springs. Dots are scaled by spring yield and coloured by temperature. The two red triangles (highest temperature) correspond to the Belham Wells (MBV1 and MBV2) at 31 °C. The inset shows the springs in the wider island context and includes Hot Water Pond (at ~56 °C) on the west coast.

Since the eruption, access to the deeper groundwater system is limited to the wells in the Belham Valley. Water emerges from the confined aquifer at 31.0 °C and 663  $\mu\text{S}/\text{cm}$  from the flowing artesian MBV2 and 31.1 °C and 630  $\mu\text{S}/\text{cm}$  from the pumped MBV1. A temperature logger installed at 65 m depth (~30 m bmsl) in the test well adjacent to MBV1 recorded consistent temperatures between 30.6 and 30.9 °C between November 2011 and February 2013.

An important component of the hydrology of Montserrat is its hydrothermal system, which is currently under investigation for geothermal energy production (Younger, 2010; Ryan et al., 2013). Apart from the inaccessible fumaroles on SHV, the hottest groundwater manifestation in the island is Hot Water Pond (HWP), north of the old capital, Plymouth. During visits in 1991 and 1992, Chiodini et al. (1996) identified several seeps supplying HWP, approximately 200 m inland, up Sand Ghaut. They encountered water close to 90 °C, with total discharges approaching 5 L/s. These seeps appear to have been buried by subsequent volcanic deposits. Satellite images indicate that the pond all but completely disappeared between May 14 and June 24 in 2006, a time period that spans the May 20 dome collapse; one of the largest dome collapse events of the eruption (Loughlin et al., 2010): a 17 km high co-ignimbritic plume deposited significant amounts of ash (up to 60 cm) in the catchment of Sand Ghaut (SAC, 2006). During visits in February 2011 and 2013 Hot Water Pond was dry. Groundwater was encountered at 50 cm depth beneath fine, reworked river and coastal sands within the dry channel of Sand Ghaut in two locations 50 m apart. SEC measurements indicate that this groundwater is likely mixed with seawater. This is confirmed by a decrease in SEC and increase in temperature between the seaward site and the up-valley site, from 40 °C and 91% of seawater SEC to 56 °C and 71% of seawater SEC. The seaward site is at the most coastal extent of Sand Ghaut, approximately 30 m from the coast, in the lee of a 1–2 m high sand bar which prevents overland connection with the sea.

#### 4.3. Discussion of hydrological field observations

Recent studies suggest that HWP represented an outflow of a geothermal system that upwells beneath St George's Hill (Ryan et al., 2013). This upwelling is proposed to be at the intersection between a SW trending fault and the WNW fault zone that includes the Belham Valley fault.

While Belham Valley well and Sunny Spring temperatures are not as high as HWP, the waters can still be considered warm. The spatial consistency in temperature and SEC between the Belham Valley Wells confirm that they tap the same aquifer, while the temporal consistency in temperature in the test well indicates that the aquifer is substantially buffered from atmospheric fluctuations and seasonal recharge variations.

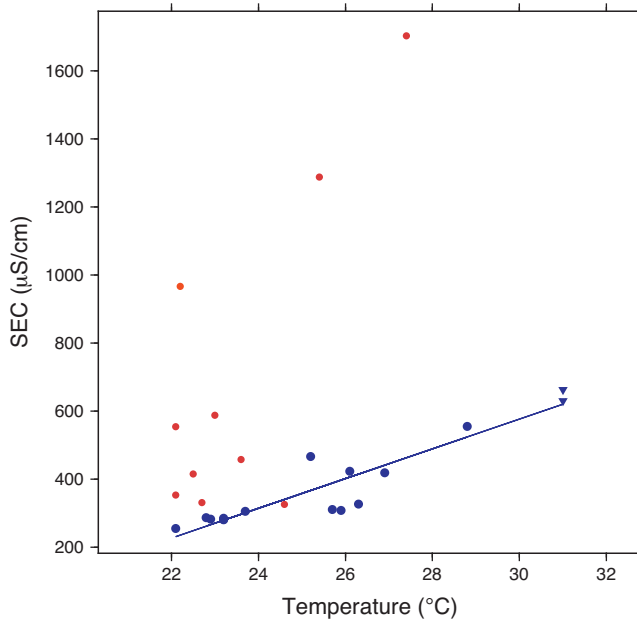


**Fig. 17.** Comparison of temperature and conductivity of the CH spring waters and the Belham well waters (triangles). Fast flowing springs clearly emanating from rocks are marked by blue dots. Slow flowing seeps and flows from boggy springs from are represented by the brown dots. The red dot represents the Monkey side spring (MkRHS) which has anomalously low temperatures and high conductivity compared to the rest of the springs in that locality; it is also highly acidic (pH  $3.51$  compared to pH  $7.44 \pm 0.9$  for all other springs). The least squares best fit of the “blue” springs is given by the equation  $C = 43.66T - 733.24$  with an  $R^2$  of  $0.86$ , where  $C$  is SEC in  $\mu\text{S}/\text{cm}$  and  $T$  is temperature in  $^\circ\text{C}$ .

It is possible that the low elevation, higher temperature, and high SEC Sunny Spring taps a similar confined aquifer, with flow through natural fracture pathways, possibly associated with the Belham Valley fracture network (Fig. 1). SEC of  $1703 \mu\text{S}/\text{cm}$  suggests some component of mixing with more conductive waters, possibly sea water; spring water SEC is 3% of local seawater conductivity.

Interestingly, the temperature of the northern and western CH springs is lower than the local ambient annual average temperature of  $25.9^\circ\text{C}$  (see Fig. 2) indicating that recharge occurs at a lower temperature. Spring temperatures lower than ambient air temperatures are not uncommon in volcanic terrain and are normally attributed to recharge occurring at higher elevation (e.g. Nathenson et al., 2003). Using the estimate of  $0.6^\circ\text{C}$  temperature decrease per 100 m elevation (Blume et al., 1974), the average temperature at a recharge elevation between 400 and 700 m amsl would be between  $21.7$  and  $23.5^\circ\text{C}$ . Spring temperatures of  $22$ – $24^\circ\text{C}$  are consistent with this.

CH spring temperatures reported here are consistent with data from previous studies (Jones et al., 2010; Chiodini et al., 1996; Davies and Peart, 2003), however previous authors have not commented on the anomalous temperatures in the southern CH springs. The warmer springs are those closest to the active SHV; however, at elevations above 190 m (over 250 m, excluding Bessy Mack) and more than 4 km from the active vent the mechanism for this local but systematic elevation of temperature is unclear. One possible mechanism is a contribution from a deeper, hotter fluid component delivered through a fracture network from a deeper aquifer. The potential of this mechanism is supported by our SEC measurements; SEC in the warmer springs is slightly elevated, compared to the western springs, towards the level observed in the deep Belham well aquifer (Fig. 17). A number of the lower yielding springs in the north also display higher SEC, but these springs are fed by slow flowing seeps emanating through soils.

## 5. Aquifer properties

### 5.1. Core scale permeability measurements

A series of 200 m deep boreholes, drilled for geophysical installation as part of the CALIPSO project (Mattioli et al., 2004), provide rare access to the geology beneath Montserrat's forested and highly weathered surface. Permeability measurements were made on 16 one-inch-diameter (2.54 cm) core samples of various lithology collected from depths ranging from 27 to 151 m in the Trants CALIPSO borehole (TRNT in Fig. 1). Five samples were tested in a liquid permeameter at constant flow rate and confining pressure of 2 MPa to simulate approximate lithostatic conditions. Pressure restrictions of the permeameter and the fragility of the samples meant that upstream pressure was limited to 700 kPa. Flow through some lower permeability samples was not possible at these pressures. Thirteen samples were tested on a gas permeameter at constant pressure.

#### 5.1.1. Core scale permeability results and discussion

Permeability of samples from TRNT range from  $3 \times 10^{-18}$  to  $6 \times 10^{-13}$  m<sup>2</sup> (Table 4). The geometric mean of the 16 core samples tested is  $7 \times 10^{-15}$  m<sup>2</sup>. Two samples were tested on both the liquid and gas permeameter. Gas permeability ( $k_{gas}$ ) measurements were higher than the liquid permeability ( $k_{liq}$ ) estimates for both samples. For the higher permeability SSK21143A,  $k_{gas} = 2k_{liq}$ . For the less permeable SSK21149A,  $k_{gas} = 3.5k_{liq}$ . The expected  $k_{gas}/k_{liq}$  ratio, due to the Klinkenberg effect of gas slippage, is  $< 2$ , for sedimentary rocks with  $k_{liq} > 10^{-16}$  m<sup>2</sup> and 2 for when  $k_{liq} < 10^{-16}$  m<sup>2</sup> (Tanikawa and Shimamoto, 2006). Other mechanisms may contribute to increased discrepancy between liquid and gas permeability, particularly in samples containing clay (Faulkner and Rutter, 2000). Gas permeability of dried samples containing clays like smectite will be higher than liquid permeability of saturated samples due to the swelling. However, agreement to within half an order of magnitude for separate permeability measurements is probably in line the tests' repeatability tolerance. While this makes it difficult to assign any discrepancy to gas slippage effects or clay swelling it does provide justification for interpreting liquid and gas measurements together.

Though identifying the deposit type that the samples are derived from is difficult, we have subdivided them into three broad types: Lava, Block and Ash, and Lahar (Fig. 18). The 10 samples categorised as Block and Ash are predominantly monolithic, containing fragments of andesite lava in a crystal rich to fine silt matrix. The Block and Ash samples show great variation in measured permeability, ranging from  $3 \times 10^{-18}$  to  $4 \times 10^{-13}$  m<sup>2</sup> with a geometric mean of  $4 \times 10^{-15}$  m<sup>2</sup>. Lahar deposit samples are distinguished from Block and Ash by their polyolithic nature, containing fragments of pumice as well as differently types (colours) of lava. The lahar samples tested have a geometric mean permeability

**Table 4**

Core sample permeability measurements. Sample codes are British Geological Survey (BGS) sample numbers.

Sample code	Depth (m)	Lithology type	Sample description	$k_{liq}$ (m <sup>2</sup> )	$k_{gas}$ (m <sup>2</sup> )
SSK21143A	26.8	Lava	Vesiculated, mafic	$2 \times 10^{-13}$	$4 \times 10^{-13}$
SSK21144A	28.3	Lava	Vuggy, vesiculated, mafic		$6 \times 10^{-13}$
SSK21147A	48.5	Block and Ash	Coarse, crystal rich matrix	$3 \times 10^{-14}$	
SSK21148A	50.3	Block and Ash	Fine, altered matrix, fractured		$3 \times 10^{-14}$
SSK21148B	50.3	Block and Ash	Fine, altered matrix	$5 \times 10^{-17}$	
SSK21149A	50.3	Block and Ash	Crystal rich matrix	$2 \times 10^{-14}$	$7 \times 10^{-14}$
SSK21149B	50.3	Block and Ash	Crystal rich matrix		$6 \times 10^{-14}$
SSK21150A	62.5	Lava	Andesite		$4 \times 10^{-17}$
SSK21151A	64.9	Lava	Andesite		$3 \times 10^{-15}$
SSK21153A	83.8	Block and Ash	Fragmented andesite, fine matrix		$5 \times 10^{-16}$
SSK21153B	83.8	Block and Ash	Fragmented andesite, fine matrix	$3 \times 10^{-18}$	
SSK21154B	86.0	Block and Ash	Heavily altered		$3 \times 10^{-16}$
SSK21155A	86.3	Block and Ash	Fragmented andesite, altered rims		$4 \times 10^{-14}$
SSK21159B	97.5	Lahar	Coarse, gravelly matrix		$2 \times 10^{-13}$
SSK21162	133.8	Lahar	Coarse, unsorted		$2 \times 10^{-14}$
SSK21165A	150.6	Block and Ash	Ash		$4 \times 10^{-13}$

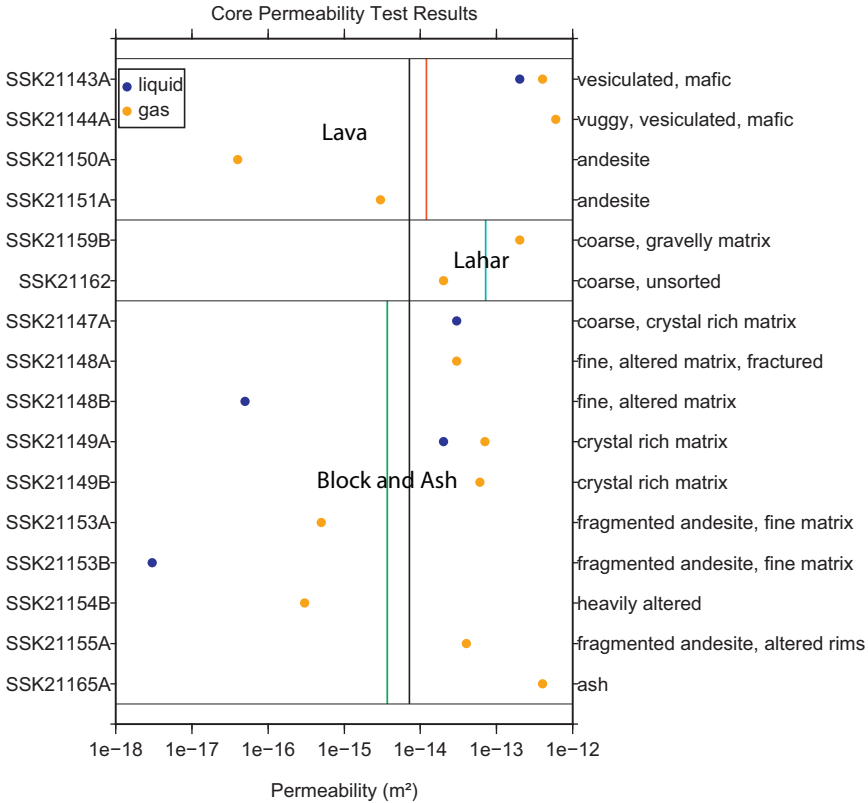


**Fig. 18.** Permeability of samples from TRNT borehole. Vertical lines correspond to geometric mean permeability for each type (Lava (red) =  $1 \times 10^{-14} \text{ m}^2$ , Lahar (light blue) =  $7 \times 10^{-14} \text{ m}^2$ , Block and Ash (green) =  $4 \times 10^{-15} \text{ m}^2$ ). The geometric mean for all 16 samples ( $7 \times 10^{-15} \text{ m}^2$ ) is also plotted (black line). Blue dots correspond to liquid permeameter measurements. Orange dots are gas permeameter measurements.

$7 \times 10^{-14} \text{ m}^2$ . Lava refers to the samples that are composed of a single crystalline lava block. The four samples are of two very different types. The lavas from 27 and 28 m depth are highly vesiculated mafic clasts with geometric mean (gas) permeability of  $5 \times 10^{-13} \text{ m}^2$ ; the more andesitic clasts from 62 to 65 m depth have a significantly lower geometric mean gas permeability of  $3 \times 10^{-16} \text{ m}^2$ .

There is no discernible relationship between permeability and sample depth, suggesting that the sample lithology is the most important factor determining permeability. Of the volcanoclastic samples, cores with higher permeabilities (above  $1 \times 10^{-14} \text{ m}^2$ ) are generally those with a matrix composed of coarser, less altered crystals or those that contain fractures. Cores with finer, more altered matrix material tend to exhibit reduced permeabilities, below  $1 \times 10^{-15} \text{ m}^2$ .

Resources were limited to providing permeability tests for samples from just one borehole. The limited number of samples restricts the statistical significance of observable trends of permeability. Further permeability test on the four other CALIPSO borehole cores would improve robustness of any observed trends in permeability. The 16 samples tested here were originally from a larger subset of cores selected for permeability tests. However, a number of the cores were too fragile and friable to be reliably tested. Although some are still quite fragile, the set of 16 samples tested represents the more consolidated and competent of samples. This generates a sampling bias towards samples that are most suitable for the tests and may result in a slight bias towards lower permeabilities, particularly in the volcanoclastic samples (Block and Ash and Lahar).

Our permeability measurements on lava samples are comparable with measurements made on dome rocks and lava from Montserrat by Melnik and Sparks (2002), who measured permeabilities between  $6 \times 10^{-16}$  and  $5 \times 10^{-12} \text{ m}^2$  on 15 cores of juvenile lava. They cite interconnected vesicles as responsible for much of the porosity, providing high permeabilities (geometric mean of  $8 \times 10^{-14} \text{ m}^2$ ). Core-scale measurements on lava blocks from Martinique show a similar range in permeability ( $1 \times 10^{-16}$ – $4 \times 10^{-12} \text{ m}^2$ ) (Bernard et al., 2007).

Samples SSK21153A and B are from adjacent parts of the drill core but yield very different core scale permeability measurements. Such variations highlight the heterogeneity of the volcanoclastic deposits. At larger scale, groundwater flow is likely affected by heterogeneities that are not adequately captured at the core scale, such as fractures and high permeability flow channels.

## 5.2. Aquifer scale permeability estimates

HydroSource (2004) performed pumping tests on the confined aquifer in the Belham Valley soon after well installation in 2004. For MBV1 the maximum drawdown after constant pumping at a rate of 50.5 L/s for 72 h was 6.8 m. The test well, located 3 m from the pumping well, experienced a maximum drawdown of 5.1 m and MBV2 152 m away experienced a drawdown of 4.8 m. Using these results the Cooper-Jacob Straight-Line method and the Distance-Drawdown method (Cooper and Jacob, 1946) give transmissivity estimates of  $2 \times 10^{-3} \text{ m}^2/\text{s}$  and  $6 \times 10^{-2} \text{ m}^2/\text{s}$ , respectively. Combined with aquifer thickness estimates from the well log of  $\sim 18 \text{ m}$ , these transmissivities equate to permeabilities of  $6 \times 10^{-11} \text{ m}^2$  and  $3 \times 10^{-10} \text{ m}^2$ ; several orders of magnitude higher than the highest core scale permeabilities measured for the CALIPSO samples (Table 4 and Fig. 18). The aquifer exploited by the Belham wells is described as a probable channel of coarse gravel and weathered pebbles (HydroSource, 2004); as such the permeability is likely to be associated with large pores and not represented in the core scale samples. Such units are likely to be among the most permeable on the island.

Intermediate scale injection and slug tests on a wider range of lithologies from Guadeloupe yield lower permeability estimates, between  $2 \times 10^{-14}$  and  $5 \times 10^{-12} \text{ m}^2$  (Charlier et al., 2011). Charlier et al. (2011) report that the most permeable deposits are pumice lapilli ( $2 \times 10^{-13}$ – $5 \times 10^{-12} \text{ m}^2$ ) and the least permeable are weathered volcanic breccia ( $2 \times 10^{-14}$ – $5 \times 10^{-14} \text{ m}^2$ ). Brecciated andesitic lava flows and unweathered pyroclastic flow deposits on Guadeloupe exhibit similar permeabilities ( $7 \times 10^{-14}$ – $6 \times 10^{-13} \text{ m}^2$ ). In general, tests at larger scales reveal higher permeabilities; they have the potential to sample flow through features that cannot be captured as core scale, such as inter-connecting fractures, large voids and coarse grained deposits. This scale dependence of permeability measurements is widely recognised (Brace, 1984).

## 6. Synopsis and development of a conceptual hydrological model

### 6.1. Synopsis of new hydrological insights

Recharge models provide reasonable first-order estimates of groundwater recharge on Montserrat. A suite of models, exploring different rainfall distribution scenarios predict whole island recharge on the order of 10–20% of rainfall with a best estimate of 266 mm/year. The models also identify strong seasonal recharge variations; over 70% of the annual recharge occurs between July and December. The models also highlight a strong land use influence; under equal rainfall and evaporation conditions, recharge is 5 times higher on bare soils and volcanic deposits than in forested regions. Recharging groundwater within the flanks of CH supplies high yielding springs. Spring waters demonstrate significant and systematic, local temperature variations. Western and northern springs waters are between 22 and 24 °C; eight southern springs discharge waters at over 25 °C. Elevated temperatures and SEC in the southern springs point towards a contribution from a deeper, warmer aquifer. Permeabilities of potential aquifers on Montserrat are explored with new permeability measurements on a range of core samples. Liquid and gas permeameter measurements reveal permeabilities between  $3 \times 10^{-18}$  and  $6 \times 10^{-13} \text{ m}^2$  with a geometric mean of  $7 \times 10^{-15} \text{ m}^2$ . These measurements are consistent with previous studies on similar materials. The preceding review and new insights provide the basis for a

discussion developing a conceptual model to describe fundamental features of Montserrat's hydrology, in particular its high yielding, high elevations springs.

## 6.2. Towards a conceptual hydrological model

In the shallow sub-surface of Montserrat fractured, jointed and brecciated andesite lavas in the islands interior are flanked by high permeability volcanoclastics, allowing rapid rainfall infiltration. High infiltration capacity results in an island with little or no surface water. Recharge at elevations above 200 m feeds a number of productive springs. Downstream of the springs the resurgent water that is not captured for consumption rapidly sinks through the ephemeral stream beds. The lack of surface water, despite the deeply incised morphology, and the losing streams, suggest a relatively low lying water table.

Logs and drilling records from the existing Belham Wells about 1.5 km from the coast indicate the existence of a shallow unconfined water table aquifer within what is described as volcanic breccia. The depth to the water table is 23 m below ground surface (HydroSource, 2004). This equates to an elevation of about 12 m amsl, consistent with the observations from the older, now buried, wells in the Belham Valley (Maxim Engineering, 1995; Davies and Peart, 2003).

Both the Hawaiian model (Peterson, 1972; Ingebritsen and Scholl, 1993) and the Canary Island model (Cabrera and Custodio, 2004; Custodio, 2007) allow for such a low lying water table towards the coast. The models diverge in their conceptualisation of the hydrology towards the interior of the islands. In the Hawaiian Model (corresponding to Robins et al. (1990)'s Type 2), the water table remains at low elevation under the islands interior, and springs at higher elevation are fed by aquifers perched on ash layers and buried soils and impounded by intrusive, volcanic dykes. In the Canary Islands model (corresponding to Robins et al. (1990)'s Type 1), the occurrence of high-elevation aquifers is related to steep doming of the water table over low permeability volcanic cores, and the only truly perched aquifers are localised and small. Robins et al. (1990)'s Type 1 has previously been applied to Montserrat (Davies and Peart, 2003).

Under either regime, the presence of the springs at relatively high elevations (Fig. 13) on the flanks of CH and SHV (pre-eruption) (Fig. 12) requires the existence of lower permeability beneath the high permeability surface lithologies. The magnitude of spring yields on Montserrat suggests that the source aquifers are reasonably extensive and therefore any low permeability features must be relatively laterally continuous. Using an annual recharge of 0.27 m/yr, from our recharge model estimates, and assuming that all recharge to the spring catchment discharges at the spring site, the recharge area required to match 18 L/s production observed at Killiekrankie spring is over 2 km<sup>2</sup>. This is over 40 times the topographically defined catchment for Killiekrankie, as estimated from a digital elevation model (DEM). Even if we use a recharge close to the annual rainfall average at Hope rain gauge (2 m/yr), the necessary recharge area still over 5 times the spring's topographically defined catchment. The aquifers that supply the springs, and therefore any low permeability unit, must extend beyond the topographically defined catchment.

In a Canary Island-type (Type 1) model intrusive volcanic cores provide a laterally continuous, low permeability unit that causes the water table to dome steeply to high elevations. In the Canaries this results in the development of high elevation aquifers that are exploited by tunnels and galleries (Carracedo, 1994). It is probable that within the central cores of Montserrat's extinct volcanic complexes there exist similar, low permeability intrusive bodies that once fed the eruptions. Whilst the lateral continuity of individual magmatic conduits may be limited, they intrude through stacked domes, which themselves are likely to be higher density. Independent gravity and seismic inversions have modelled high density cores, at sea level, beneath SH and CH (Hautmann et al., 2013; Paulatto et al., 2010; Shalev et al., 2010). Unfortunately, due to issues related to occupying stations and deploying equipment within the steep sloped interior of the island, geophysical surveys have struggled to illuminate structures above sea level. It is likely, however, that high density cores do extend above sea level, into the edifice. At some depth below the surface they transition from unfractured or healed intrusive bodies to the more fractured and higher permeability extrusive and jointed shallow intrusive bodies that can be observed on the surface. Springs will form where the erosional surface intersects this transition (Fig. 19).

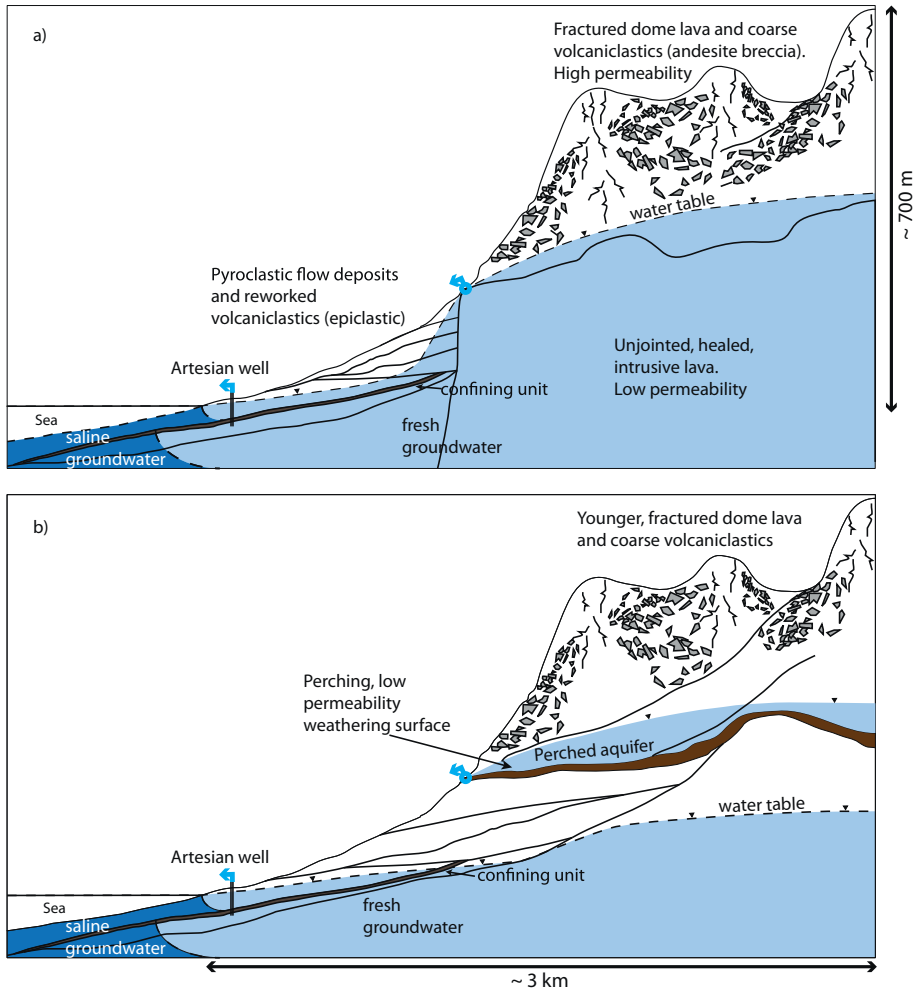


**Fig. 19.** Potential application of the Canary Island (Type 1) conceptual model (a) and the Hawaiian (Type 2) conceptual model (b) to explain CH springs and artesian coastal aquifers.

Intrusive bodies are also implicated in spring development in a Hawaiian-type (Type 2) model; intrusive dykes impound groundwater and generate perched aquifers. On Hawaii, high elevation aquifers are also perched by ash layers. Ash layers on Montserrat tend to be thin; tephra-fallout deposits associated with the first 4 years of eruption reached maximum accumulation of 43 cm (Bonadonna et al., 2002). Preserved ash layers around CH are infrequent, with maximum thicknesses of around 20 cm. Such compacted ash layers are likely to be low permeability and they may present localised perching units, capable of compartmentalising groundwater flow. However, their limited thickness and lack of lateral continuity restricts their ability to perch aquifers of the scale required to supply the springs on Montserrat.

On Montserrat there exist other volcanic deposits that are intrinsically low permeability. Such units are associated with both high temperature and low temperature weathering and alteration. The Soufrière on SHV testify to the prevalence of the hydrothermal system on the active volcano. Hydrothermal alteration is a function of fluid-rock interaction at elevated pressure and temperature. Common alteration occurring in such systems includes precipitation of silica polymorphs and

sulphates by acid waters, often proximal to fumarolic vents (Boudon et al., 1998). Less acid systems are associated with mineral breakdown to clays such as smectite and kaolinite (Giggenbach, 1988). Boudon et al. (1998) estimate that the silica alteration zone, delineated by the active soufrières extends to a diameter of ~2 km around the centre of SHV and is coupled with precipitation and infilling of pores and fractures with amorphous and microcrystalline silica. An extensive silica alteration zone, coupled with significant clay alteration associated with low temperature alteration and meteoric weathering, could potentially lead to the development of a low permeability surface layer. If this surface is buried by subsequent eruptive deposits it has the potential to provide a large, laterally continuous aquitard. Subsequent downcutting of the ghauts to intersect the aquitard will promote the formation of springs (Fig. 19).

Type 2 differs from Type 1 in that aquifers supplying the high elevation springs are perched or impounded within a vadose zone that is several hundreds of metres thick. Under this regime the units beneath the perching aquitard would be unsaturated. An unpublished commercial report (Maxim Engineering, 1995) states that a 1967/1968 water test well located in a ghaut on the northern slopes of CH at ~200 m amsl was drilled to a depth of 75 m amsl and did not encounter saturated material. Up-valley of this drill site at the elevations of 315 and 345 m amsl the ghaut is fed by Blackwood Allan and Mongo Springs.

In the Type 2 model the spring aquifers are hydraulically connected to the deeper hydrological system and to low elevation coastal aquifers. Under these conditions spring behaviour, temperature and composition is hydraulically coupled with groundwater conditions and pressure at depth, and therefore to volcanic perturbation. By defining hydraulic connectivity between low and high elevation aquifers, this model can better explain the anomalously warm springs at high elevation on the south side of CH.

Certain observations from Montserrat are consistent with either of the major volcanic island conceptual hydrology models. Without deep boreholes within the central portions of Montserrat's volcanic complexes it is difficult to definitively propose which model best represents the hydrology of this volcanic arc island. Both should be maintained as working hypotheses, with a view to gathering data to better constrain the system.

## 7. Conclusions

High yielding springs on the flanks of the extinct Centre Hills volcanic complex and low lying aquifers in more distal locations provide an essential water resource to the island's population, as it recovers from over 15 years of volcanic activity. Recharge models predict annual recharge of 10–20% of annual rainfall with a strong seasonality; models predict that over 70% of the islands recharge occurs between July and December. Land use is a critical control on recharge; during extended periods of quiescence changes in vegetation type, including colonisation and eventual afforestation of young deposits in the south, and deforestation for agriculture around Centre Hills, are expected to modify the current recharge conditions. Recharge will also be affected by any fluctuations in rainfall patterns associated with climate change; this will, no doubt, have implications for spring yield.

The development of springs at elevations of 200–400 m amsl, on an island with only ephemeral rivers and no other surface water, requires the presence of low permeability units. Assuming a recharge rate of 0.27 m/yr the surface recharge area required to supply the highest yielding spring on Montserrat is over 40 times the topographically defined catchment. This suggests that the low permeability bodies responsible for raising the water table to the elevation of the springs must be reasonably laterally extensive.

A suite of core-scale permeability tests reveal permeabilities between  $3 \times 10^{-18}$  and  $6 \times 10^{-13}$  m<sup>2</sup> for samples of lava and volcanoclastic deposits. Generally, coarser and less altered samples demonstrate higher permeabilities ( $>10^{-14}$  m<sup>2</sup>), while cores with finer and altered matrix material exhibit permeabilities below  $10^{-15}$  m<sup>2</sup>. Andesitic lava samples also reveal low permeabilities, on the order of  $10^{-16}$  m<sup>2</sup>. Analysis of a previous pumping test on a confined aquifer in Montserrat's Belham valley reveal aquifer permeability of  $10^{-10}$  m<sup>2</sup>.

New insights and observations from Montserrat combined with a review of existing understanding of hydrologic on volcanic islands provides the basis for a discussion on potential conceptual

hydrological models for Montserrat, specifically the Centre Hills springs. Current observations from Montserrat are consistent with two possible conceptual hydrological models for volcanic island settings. Type 1 resembles the model applied to the Canary Islands; a low permeability core within the interior of the island elevates the water table allowing the development of aquifers and springs at high elevation. Type 2 is based on a conceptual model devised for Hawaii; springs are supplied by perched aquifers above low permeability, weathered aquitard.

The hydrology of Montserrat is further complicated by the active volcanic system in the south. This link is not restricted to fumaroles on the flanks of the active SHV; high temperature, low elevation springs at Hot Water Pond suggest that volcanic influence on the hydrology extends to the east coast, some 6 km from the active vent. Elevated temperatures and SEC in the southern springs on CH point towards a contribution from warmer waters potentially supplied through faults from a warmer aquifer at depth.

The insights presented here provide useful constraints for numerical simulations to explore the fundamental hydrology of Montserrat, and distinguish which of these two conceptual models best represents Montserrat's hydrological system and the hydrology of volcanic arc islands in general. Improving our understanding of fundamental hydrology of such islands is essential for exploring hydrological and volcanic interactions as well as assessing the behaviour of a vital resource in response to a changing climate.

### Conflict of interest

None declared.

### Acknowledgements

The authors would like to thank MUL, Montserrat for providing access to their data archive and assistance in the field. In particular, this work was made possible by invaluable field support and guidance from Reuel Lee and Bill Tonge (formerly MUL). We are also grateful for assistance and contributions from a number of MVO staff and for assistance in the field from Alia Jasim (UOB). Thanks also to Jenni Barclay and Adrian Matthew for sharing rainfall data, and Steve Sparks for allowing access to CALIPSO cores. This work is funded by the NERC BUFI programme (studentship no. S186) and has benefited from interaction and collaboration with many BGS staff; particular thanks are due to Andrew Butcher and Majdi Mansour. This work also benefited from funding from The Royal Society, EC-FP7 (#282759) "VUELCO", and the NERC [NE/E007961/1]. Hughes publishes with the permission of the Executive Director of BGS (NERC). The authors would also like to thank Nicolas Fournier and Steve Ingebritsen for insightful and constructive reviews that have helped to improve the manuscript.

### Appendix A.

#### Table TableA.1

**TableA.1**

Springs documented in Walker (1965). Spring codes used in Figs. 12–14.

Spring code	Spring name	Lat. (° N)	Lon. (° W)	Alt. (m)
AmA	Amersham A	16.70411	62.19940	168
AmB	Amersham B	16.70665	62.19612	213
AmC	Amersham C	16.70801	62.19368	290
AmD	Amersham D	16.70521	62.19302	351
BRB	Big River B	16.76252	62.19289	309
BRC	Big River C	16.76651	62.18783	302
Ba	Bath	16.72699	62.20074	169
CRL	Cold River Lower	16.71211	62.15635	114
CRU	Cold River Upper	16.71184	62.15710	115
Cn	Central	16.76361	62.19158	385

Table A.1 (Continued)

Spring code	Spring name	Lat. (° N)	Lon. (° W)	Alt. (m)
Dw	Dowdie	16.69727	62.17360	539
Gd	Gadinge	16.70224	62.17595	577
HR	Hot River	16.71671	62.16161	195
NR	New River	16.71923	62.18019	494
Ro	Roches	16.70207	62.16347	323
Ry	Ryan	16.69862	62.17613	500
Sp	Sappit	16.74904	62.20377	274
WR	White River	16.70133	62.17735	396

## References

- Barclay, J., Alexander, J., Susnik, J., 2007. Rainfall-induced lahars in the Belham Valley, Montserrat, West Indies. *J. Geol. Soc. Lond.* 164, 815–827, <http://dx.doi.org/10.1144/0016-76492006-078>.
- Barclay, J., Johnstone, J.E., Matthews, A.J., 2006. Meteorological monitoring of an active volcano: implications for eruption prediction. *J. Volcanol. Geotherm. Res.* 150, 339–358, <http://dx.doi.org/10.1016/j.jvolgeores.2005.07.020>.
- Bernard, M.L., Zamora, M., Géraud, Y., Boudon, G., 2007. Transport properties of pyroclastic rocks from Montagne Pelée volcano (Martinique Lesser Antilles). *J. Geophys. Res.* 112, 1–16, <http://dx.doi.org/10.1029/2006JB004385>.
- Blume, H., Maczewski, J., Norton, A., 1974. *The Caribbean Islands*. Longman, London.
- Bonadonna, C., Mayberry, G.C., Calder, E.S., Sparks, R.S.J., Choux, C., Jackson, P., Lejeune, A.M., Loughlin, S.C., Norton, G.E., Rose, W.I., Ryan, G., Young, S.R., 2002. Tephra fallout in the eruption of Soufriere Hills Volcano, Montserrat. *Geol. Soc. Lond. Mem.* 21, 483–516, <http://dx.doi.org/10.1144/GSL.MEM.2002.021.01.22>.
- Boudon, G., Villemant, B., Komorowski, J.C., Ildefonse, P., Semet, M.P., 1998. The hydrothermal system at Soufriere Hills Volcano, Montserrat (West Indies): characterization and role in the on-going eruption. *Geophys. Res. Lett.* 25, 3693–3696, <http://dx.doi.org/10.1029/98GL00985>.
- Brace, W.F., 1984. Permeability of crystalline rocks: new in situ measurements. *J. Geophys. Res.* 89, 4327, <http://dx.doi.org/10.1029/JB089iB06p04327>.
- Cabrera, M., Custodio, E., 2004. Groundwater flow in a volcanic-sedimentary coastal aquifer: Telde area, Gran Canaria, Canary Islands, Spain. *Hydrogeol. J.* 12, 305–320, <http://dx.doi.org/10.1007/s10040-003-0316-y>.
- Carracedo, J., 1994. The Canary Islands: an example of structural control on the growth of large oceanic-island volcanoes. *J. Volcanol. Geotherm. Res.* 60, 225–241, [http://dx.doi.org/10.1016/0377-0273\(94\)90053-1](http://dx.doi.org/10.1016/0377-0273(94)90053-1).
- Cassidy, M., Taylor, R.N., Palmer, M.R., Cooper, R.J., Stenlake, C., Trofimovs, J., 2012. Tracking the magmatic evolution of island arc volcanism: insights from a high-precision Pb isotope record of Montserrat, Lesser Antilles. *Geochem. Geophys. Geosyst.* 13, Q05003, <http://dx.doi.org/10.1029/2012GC004064>.
- Charlier, J.B., Lachassagne, P., Ladouche, B., Cattani, P., Moussa, R., Voltz, M., 2011. Structure and hydrogeological functioning of an insular tropical humid andesitic volcanic watershed: a multi-disciplinary experimental approach. *J. Hydrol.* 398, 155–170, <http://dx.doi.org/10.1016/j.jhydrol.2010.10.006>.
- Chiodini, G., Cioni, R., Frullani, A., Guidi, M., Marini, L., Prati, F., Raco, B., 1996. Fluid geochemistry of Montserrat Island, West Indies. *Bull. Volcanol.* 58, 380–392, <http://dx.doi.org/10.1007/s004450050146>.
- Cole, P.D., Calder, E.S., Druitt, T.H., Hoblitt, R., Robertson, R., Sparks, R.S.J., Young, S.R., 1998. Pyroclastic flows generated by gravitational instability of the 1996–97 Lava Dome of Soufriere Hills Volcano, Montserrat. *Geophys. Res. Lett.* 25, 3425–3428, <http://dx.doi.org/10.1029/98GL01510>.
- Cole, P.D., Calder, E.S., Sparks, R.S.J., Clarke, A.B., Druitt, T.H., Young, S.R., Herd, R.A., Harford, C.L., Norton, G.E., 2002. Deposits from dome-collapse and fountain-collapse pyroclastic flows at Soufriere Hills Volcano, Montserrat. *Geol. Soc. Lond. Mem.* 21, 231–262, <http://dx.doi.org/10.1144/GSL.MEM.2002.021.01.11>.
- Cooper, H.H., Jacob, C.E., 1946. A generalized graphical method for evaluating formation constants and summarizing well-field history. *Trans. Am. Geophys. Union* 27, 526, <http://dx.doi.org/10.1029/TR027i004p00526>.
- Cruz, V., Silva, O., 2001. Hydrogeologic framework of Pico Island, Azores, Portugal. *Hydrogeol. J.* 9, 177–189, <http://dx.doi.org/10.1007/s100400000106>.
- Custodio, E., 2007. Groundwater in volcanic hard rocks. In: Krásný, J., Sharp, J.M. (Eds.), *Groundw. Fract. Rocks IAH Sel. Pap. Ser. Taylor and Francis*, pp. 95–108, <http://dx.doi.org/10.1201/9780203945650.ch5> (Chapter 5).
- Davies, J., Peart, R., 2003. *A Review of the Groundwater Resources of Central and Northern Montserrat. Technical Report CR/03/257C*. British Geological Survey.
- Donnelly, L., 2007. Engineering geology of landslides on the volcanic island of Montserrat, West Indies. *Quart. J. Eng. Geol. Hydrogeol.* 40, 267–292, <http://dx.doi.org/10.1144/1470-9236/06-039>.
- Druitt, T.H., Young, S.R., Bapptie, B., Bonadonna, C., Calder, E.S., Clarke, A.B., Cole, P.D., Harford, C.L., Herd, R.A., Luckett, R., Ryan, G., Voigt, B., 2002. Episodes of cyclic Vulcanian explosive activity with fountain collapse at Soufriere Hills Volcano, Montserrat. *Geol. Soc. Lond. Mem.* 21, 281–306, <http://dx.doi.org/10.1144/GSL.MEM.2002.021.01.13>.
- Ecker, A., 1976. Groundwater behaviour in Tenerife, volcanic island (Canary Islands, Spain). *J. Hydrol.* 28, 73–86, [http://dx.doi.org/10.1016/0022-1694\(76\)90053-6](http://dx.doi.org/10.1016/0022-1694(76)90053-6).
- Faulkner, D.R., Rutter, E.H., 2000. Comparisons of water and argon permeability in natural clay-bearing fault gouge under high pressure at 20C. *J. Geophys. Res.* 105, 16415, <http://dx.doi.org/10.1029/2000JB900134>.
- Feuillet, N., Leclerc, F., Tapponnier, P., Beauducel, F., Boudon, G., Le Friant, A., Deplus, C., Lebrun, J.F., Nercessian, A., Saurel, J.M., Clément, V., 2010. Active faulting induced by slip partitioning in Montserrat and link with volcanic activity: new insights from the 2009 GWADASEIS marine cruise data. *Geophys. Res. Lett.* 37, <http://dx.doi.org/10.1029/2010GL042556>.

- Fisher, R.V., Heiken, G., Mazzoni, M., 2006. Chapter 2.1 Where do tuffs fit into the framework of volcanoes? *Geol. Soc. Am. Spec. Pap.* 408, 5–9, [http://dx.doi.org/10.1130/2006.2408\(2.1\)](http://dx.doi.org/10.1130/2006.2408(2.1)).
- Fournier, N., Moreau, M., Robertson, R., 2010. Disappearance of a crater lake: implications for potential explosivity at Soufrière volcano, St Vincent, Lesser Antilles. *Bull. Volcanol.* 73, 543–555, <http://dx.doi.org/10.1007/s00445-010-0422-3>.
- Germanovich, L.N., Lowell, R.P., 1995. The mechanism of phreatic eruptions. *J. Geophys. Res.* 100, 8417, <http://dx.doi.org/10.1029/94JB03096>.
- Giggenbach, W.F., 1988. Geothermal solute equilibria. Derivation of Na–K–Mg–Ca geothermometers. *Geochim. Cosmochim. Acta* 52, 2749–2765, [http://dx.doi.org/10.1016/0016-7037\(88\)90143-3](http://dx.doi.org/10.1016/0016-7037(88)90143-3).
- Harford, C.L., Pringle, M.S., Sparks, R.S.J., Young, S.R., 2002. The volcanic evolution of Montserrat using 40Ar/39Ar geochronology. *Geol. Soc. Lond. Mem.* 21, 93–113, <http://dx.doi.org/10.1144/GSL.MEM.2002.021.01.05>.
- Hautmann, S., Camacho, A.G., Gottsmann, J., Odbert, H.M., Syers, R.T., 2013. The shallow structure beneath Montserrat (West Indies) from new Bouguer gravity data. *Geophys. Res. Lett.* 40, 5113–5118, <http://dx.doi.org/10.1002/grl.51003>.
- Hautmann, S., Gottsmann, J., Camacho, A.G., Fournier, N., Sacks, I.S., Sparks, R.S.J., 2010. Mass variations in response to magmatic stress changes at Soufrière Hills Volcano, Montserrat (W.I.): insights from 4-D gravity data. *Earth Planet. Sci. Lett.* 290, 83–89, <http://dx.doi.org/10.1016/j.epsl.2009.12.004>.
- Hautmann, S., Gottsmann, J., Sparks, R.S.J., Costa, A., Melnik, O., Voight, B., 2009. Modelling ground deformation caused by oscillating overpressure in a dyke conduit at Soufrière Hills Volcano, Montserrat. *Tectonophysics* 471, 87–95, <http://dx.doi.org/10.1016/j.tecto.2008.10.021>.
- Heilweil, V.M., Solomon, D.K., Gingerich, S.B., Verstraeten, I.M., 2009. Oxygen, hydrogen, and helium isotopes for investigating groundwater systems of the Cape Verde Islands, West Africa. *Hydrogeol. J.* 17, 1157–1174, <http://dx.doi.org/10.1007/s10040-009-0434-2>.
- Hughes, A.G., Mansour, M.M., Robins, N.S., 2008. Evaluation of distributed recharge in an upland semi-arid karst system: the West Bank Mountain Aquifer, Middle East. *Hydrogeol. J.* 16, 845–854, <http://dx.doi.org/10.1007/s10040-008-0273-6>.
- Hurwitz, S., Johnston, M.J.S., 2003. Groundwater level changes in a deep well in response to a magma intrusion event on Kilauea Volcano, Hawai'i. *Geophys. Res. Lett.* 30, 2173, <http://dx.doi.org/10.1029/2003GL018676>.
- HydroSource, 2004. *Groundwater Exploration and Development of High Yield Water Supply Wells for The Montserrat Water Authority. Technical Report. Hydrosource Assoc. Inc., Ashland, New Hampshire.*
- Ingebritsen, S., Scholl, M., 1993. The hydrogeology of Kilauea volcano. *Geothermics* 22, 255–270, [http://dx.doi.org/10.1016/0375-6505\(93\)90003-6](http://dx.doi.org/10.1016/0375-6505(93)90003-6).
- Join, J.L., Folio, J.L., Robineau, B., 2005. Aquifers and groundwater within active shield volcanoes. Evolution of conceptual models in the Piton de la Fournaise volcano. *J. Volcanol. Geotherm. Res.* 147, 187–201, <http://dx.doi.org/10.1016/j.jvolgeores.2005.03.013>.
- Jones, M.T., Hembury, D.J., Palmer, M.R., Tonge, B., Darling, W.G., Loughlin, S.C., 2010. The weathering and element fluxes from active volcanoes to the oceans: a Montserrat case study. *Bull. Volcanol.* 73, 207–222, <http://dx.doi.org/10.1007/s00445-010-0397-0>.
- Keller, G.V., Grose, L., Murray, J.C., Skokan, C.K., 1979. Results of an experimental drill hole at the summit of kilauea volcano, Hawaii. *J. Volcanol. Geotherm. Res.* 5, 345–385, [http://dx.doi.org/10.1016/0377-0273\(79\)90024-6](http://dx.doi.org/10.1016/0377-0273(79)90024-6).
- Kenedi, C.L., Sparks, R.S.J., Malin, P., Voight, B., Dean, S., Minshull, T., Paulatto, M., Peirce, C., Shalev, E., 2010. Contrasts in morphology and deformation offshore Montserrat: new insights from the SEA-CALIPSO marine cruise data. *Geophys. Res. Lett.* 37, 1–7, <http://dx.doi.org/10.1029/2010GL043925>.
- Kopylova, G.N., Boldina, S.V., 2012. On the relationships of water-level variations in the E-1 well, Kamchatka to the 2008–2009 resumption of activity on Koryakskii volcano and to large (M 5) earthquakes. *J. Volcanol. Seismol.* 6, 316–328, <http://dx.doi.org/10.1134/S0742004631205003X>.
- Le Friant, a., Harford, C., Deplus, C., Boudon, G., Sparks, R., Herd, R., Komorowski, J., 2004. Geomorphological evolution of Montserrat (West Indies): importance of flank collapse and erosional processes. *J. Geol. Soc. Lond.* 161, 147–160, <http://dx.doi.org/10.1144/0016-764903-017>.
- Loughlin, S.C., Luckett, R., Ryan, G., Christopher, T., Hards, V., De Angelis, S., Jones, L., Strutt, M., 2010. An overview of lava dome evolution, dome collapse and cyclicity at Soufrière Hills Volcano, Montserrat, 2005–2007. *Geophys. Res. Lett.* 37, 4–9, <http://dx.doi.org/10.1029/2010GL042547>.
- Mansour, M.M., Barkwith, A., Hughes, A.G., 2011. A simple overland flow calculation method for distributed groundwater recharge models. *Hydro. Process.* 25, 3462–3471, <http://dx.doi.org/10.1002/hyp.8074>.
- Mattioli, G.S., Young, S.R., Voight, B., Steven, R., Sparks, J., Shalev, E., Sacks, S., Malin, P., Linde, A., Johnston, W., Hidayat, D., Elsworth, D., Dunkley, P., Herd, R., Neuberger, J., Norton, G., Widiwijayanti, C., 2004. Prototype PBO instrumentation of CALIPSO project captures world-record lava dome collapse on Montserrat Volcano. *Eos Trans. Am. Geophys. Union* 85, 317, <http://dx.doi.org/10.1029/2004EO340001>.
- Maxim Engineering, Inc., 1995. *Belham Valley Water Supply Site Investigation Report, Technical Report. Maxim Engineering Inc., Edmonton, Alberta, Canada.*
- Melnik, O., Sparks, R.S.J., 2002. Dynamics of magma ascent and lava extrusion at Soufrière Hills Volcano, Montserrat. *Geol. Soc. Lond. Mem.* 21, 153–171, <http://dx.doi.org/10.1144/GSL.MEM.2002.021.01.07>.
- Nathenson, M., Thompson, J., White, L., 2003. Slightly thermal springs and non-thermal springs at Mount Shasta, California: chemistry and recharge elevations. *J. Volcanol. Geotherm. Res.* 121, 137–153, [http://dx.doi.org/10.1016/S0377-0273\(02\)00426-2](http://dx.doi.org/10.1016/S0377-0273(02)00426-2).
- Nieuwenhuys, A., Jongmans, A., van Breemen, N., 1993. Andisol formation in a Holocene beach ridge plain under the humid tropical climate of the Atlantic coast of Costa Rica. *Geoderma* 57, 423–442, [http://dx.doi.org/10.1016/0016-7061\(93\)90053-N](http://dx.doi.org/10.1016/0016-7061(93)90053-N).
- Paulatto, M., Minshull, T.a., Baptie, B., Dean, S., Hammond, J.O.S., Henstock, T., Kenedi, C.L., Kiddle, E.J., Malin, P., Peirce, C., Ryan, G., Shalev, E., Sparks, R.S.J., Voight, B., 2010. Upper crustal structure of an active volcano from refraction/reflection tomography, Montserrat, Lesser Antilles. *Geophys. J. Int.* 180, 685–696, <http://dx.doi.org/10.1111/j.1365-246X.2009.04445.x>.
- Peterson, F.L., 1972. Water development on Tropic Volcanic Islands-Type Example: Hawaii. *Ground Water* 10, 18–23, <http://dx.doi.org/10.1111/j.1745-6584.1972.tb03586.x>.

- Rad, S., Allegre, C., Louvat, P., 2007. Hidden erosion on volcanic islands. *Earth Planet. Sci. Lett.* 262, 109–124, <http://dx.doi.org/10.1016/j.epsl.2007.07.019>.
- Ramdin, R., Hosein, G., 1995. *Investigation on the Decline of Spring Production in Montserrat W.I. Technical Report. Trinidad and Tobago Water and Sewerage Authority.*
- Rea, W.J., 1974. The volcanic geology and petrology of Montserrat, West Indies. *J. Geol. Soc. Lond.* 130, 341–366, <http://dx.doi.org/10.1144/gsjgs.130.4.0341>.
- Reid, M.E., Sisson, T.W., Brien, D.L., 2001. Volcano collapse promoted by hydrothermal alteration and edifice shape, Mount Rainier, Washington. *Geology* 29, 779, [http://dx.doi.org/10.1130/0091-7613\(2001\)029<0779:VCPBHA>2.0.CO;2](http://dx.doi.org/10.1130/0091-7613(2001)029<0779:VCPBHA>2.0.CO;2).
- Robins, N.S., Lawrence, A.R., Cripps, A.C., 1990. Problems of ground-water development in small volcanic islands in the eastern Caribbean. In: *Trop. Hydrol. Caribb. Islands Water Resour. American Water Resources Association, San Juan*, pp. 257–267.
- Roobol, M.J., Smith, A.L., 1998. Pyroclastic stratigraphy of the Soufriere Hills Volcano, Montserrat – implications for the present eruption. *Geophys. Res. Lett.* 25, 3393–3396, <http://dx.doi.org/10.1029/98GL00643>.
- Ryan, G.a., Peacock, J.R., Shalev, E., Rugis, J., 2013. Montserrat geothermal system: a 3D conceptual model. *Geophys. Res. Lett.* 40, 2038–2043, <http://dx.doi.org/10.1002/grl.50489>.
- SAC, 2006. *Seventh Report of the Scientific Advisory Committee on Montserrat Volcanic Activity. Technical Report 7. Scientific Advisory Committee on Montserrat Volcanic Activity.*
- Schwartz, F.W., Zhang, H., 2003. *Fundamentals of Ground Water. John Wiley & Sons, New York.*
- Shalev, E., Kenedi, C.L., Malin, P., Voight, V., Miller, V., Hidayat, D., Sparks, R.S.J., Minshull, T., Paulatto, M., Brown, L., Mattioli, G.S., 2010. Three-dimensional seismic velocity tomography of Montserrat from the SEA-CALIPSO offshore/onshore experiment. *Geophys. Res. Lett.* 3, 7, <http://dx.doi.org/10.1029/2010GL042498>.
- Shibata, T., Akita, F., 2001. Precursory changes in well water level prior to the March, 2000 eruption of Usu Volcano, Japan. *Geophys. Res. Lett.* 28, 1799–1802, <http://dx.doi.org/10.1029/2000GL012467>.
- Sigurdsson, H., Sparks, R.S.J., Carey, S.N., Huang, T.C., 1980. Volcanogenic sedimentation in the Lesser Antilles Arc. *J. Geol.* 88, 523–540, <http://dx.doi.org/10.1086/628542>.
- Sparks, R.S.J., Barclay, J., Calder, E.S., Herd, R.A., Komorowski, J.C., Luckett, R., Norton, G.E., Ritchie, L.J., Voight, B., Woods, A.W., 2002. Generation of a debris avalanche and violent pyroclastic density current on 26 December (Boxing Day) 1997 at Soufriere Hills Volcano, Montserrat. *Geol. Soc. Lond. Mem.* 21, 409–434, <http://dx.doi.org/10.1144/GSL.MEM.2002.021.01.18>.
- Stuart, M., Maurice, L., Heaton, T., Sapiano, M., Micallef Sultana, M., Goody, D., Chilton, P., 2010. Groundwater residence time and movement in the Maltese islands: a geochemical approach. *Appl. Geochem.* 25, 609–620, <http://dx.doi.org/10.1016/j.apgeochem.2009.12.010>.
- Tanikawa, W., Shimamoto, T., 2006. Klinkenberg effect for gas permeability and its comparison to water permeability for porous sedimentary rocks. *Hydrol. Earth Syst. Sci. Discuss.* 3, 1315–1338, <http://dx.doi.org/10.5194/hessd-3-1315-2006>.
- Thomas, D.M., Paillet, F.L., Conrad, M.E., 1996. Hydrogeology of the Hawaii Scientific Drilling Project borehole KP-1: 2. Ground-water geochemistry and regional flow patterns. *J. Geophys. Res.* 101, 11683, <http://dx.doi.org/10.1029/95JB03845>.
- Thorntwaite, C.W., 1948. An approach toward a rational classification of climate. *Geogr. Rev.* 38, 55, <http://dx.doi.org/10.2307/210739>.
- Wadge, G., Herd, R., Ryan, G., Calder, E.S., Komorowski, J.C., 2010. Lava production at Soufrière Hills Volcano, Montserrat: 1995–2009. *Geophys. Res. Lett.* 3, 7, <http://dx.doi.org/10.1029/2009GL041466>.
- Walker, S., 1965. *Report on Water Resources of Montserrat. Government of Montserrat, Plymouth, Montserrat.*
- Whitaker, F.F., Smart, P.L., 1997. Hydrogeology of the Bahamian archipelago. *Dev. Sedimentol.* 54, 183–216, [http://dx.doi.org/10.1016/S0070-4571\(04\)80026-8](http://dx.doi.org/10.1016/S0070-4571(04)80026-8).
- Young, S.R., Sparks, R.S.J., Aspinall, W.P., Lynch, L.L., Miller, A.D., Robertson, R.E.A., Shepherd, J.B., 1998. Overview of the eruption of Soufriere Hills Volcano Montserrat 18 July 1995 to December 1997. *Geophys. Res. Lett.* 25, 3389–3392, <http://dx.doi.org/10.1029/98GL01405>.
- Younger, P., 2010. Reconnaissance assessment of the prospects for development of high-enthalpy geothermal energy resources, Montserrat. *Quart. J. Eng. Geol. Hydrogeol.* 43, 11–22, <http://dx.doi.org/10.1144/1470-9236/08-083>.
- Zellmer, G.F., Hawkesworth, C.J., Sparks, R.S.J., Thomas, L.E., Harford, C.L., Brewer, T.S., Loughlin, S.C., 2003. Geochemical Evolution of the Soufrière Hills Volcano, Montserrat, Lesser Antilles Volcanic Arc. *J. Petrol.* 44, 1349, <http://dx.doi.org/10.1093/petrology/44.8.1349>.